B 3 Diffusion [1]

Jan K.G. Dhont
Institut of Complex Systems ICS-3
Forschungszentrum Jülich GmbH

Contents

[1] Lecture Notes of the 43^{rd} IFF Spring School "Scattering Methods for Condensed Matter Research: Towards Novel Applications at Future Sources" (Forschungszentrum Jülich, 2012).

1 Introduction

Diffusion relates to the displacement of molecules due to their thermal motion. Diffusion is a general phenomenon that occurs in gases, fluids and solids. Clearly, the interactions between molecules affect their thermally induced displacements. In a crystalline solid, for example, a relatively small diffusing molecule is surrounded by large molecules that reside on average at their crystal lattice sites. These surrounding molecules form a "cage" within which the given small molecule moves around. Depending on the height of the energy barrier set by the interactions with the molecules forming the cage, the tagged molecule occasionally escapes from a cage and moves to a neigbouring cage. In a gas the displacement of a molecule is not hindered by a structured cage of neighbouring molecules, as in a solid. Here, occasional collisions with other molecules in this very dilute system will change the magnitude and direction of the velocity of the tagged molecule. In a fluid the diffusion mechanism is in between that of a solid and a gas: there is a "blurry cage" around each molecule, but this cage is highly dynamic itself, which enhances the cage-escape frequency.
The above described thermal motion of a single molecule in a macroscopically homogeneous system (as depicted in Fig.1a) is referred to as **self diffusion**, where "self" refers to the fact that the dynamics of a single molecule is considered. The diffusive motion of a single molecule can be quantified as follows. Consider a molecule with a prescribed position of its center-of-mass $\mathbf{r}_0$ at time $t = 0$. Let $\mathbf{r}(t)$ denote the position of the molecule at a later time t. In a macroscopically homogeneous system, on average, the probability of a displacement to the left is equal to a displacement to the right. Therefore the average displacement $< \mathbf{r}(t) - \mathbf{r}_0 >$ will be zero. Here, the brackets $< \cdots >$ denote thermal averaging, that is, averaging with respect to the probability that the position is equal to $\mathbf{r}$ at time t, given that the position is $\mathbf{r}_0$ at time $t = 0$ (we will give a precise definition of probability density functions later). The average displacement can therefore not be used to characterize the diffusive motion of a molecule. The most simple quantity that can be used for this purpose is the so-called *mean-squared displacement* $W(t)$, which is defined as,

$$W(t) \equiv <|\mathbf{r}(t) - \mathbf{r}_0|^2> \ . \tag{1}$$

Clearly this is a non-zero and non-trivial function of time.
Thermal motion of molecules leads to an overall net mass transport in case the concentration of the diffusing species varies with position (as depicted in Fig.1b for a solution of molecules, and in Fig.1c for relatively small molecules that diffuse through an essentially static environment of a crystalline solid). Mass is transported from the region of high concentration to the region of low concentration, as indicated by the arrows in Fig.1b,c. This type of diffusion process is referred to as **gradient diffusion** or **collective diffusion**, where "collective" refers to the coherent displacement of many molecules. An intuitive understanding of why net mass transport occurs due to concentration gradients is as follows. A given diffusing molecule experiences a different number of thermal collisions with neignbouring particles on the side facing the region with high concentration and that with low concentration. This results in a net force on that molecule, which therefore attains a net velocity. There are more collisions on the side where the concentration is high as compared to the side where the concentration is low, so that mass transport will typically occur towards regions of lower concentration.
A third type of diffusion process is the mixing of two (or more) molecular species, where the various species exhibit concentration gradients. Like for collective diffusion there is a net mass transport for each of the species, but the mass fluxes of the various species need not be in the

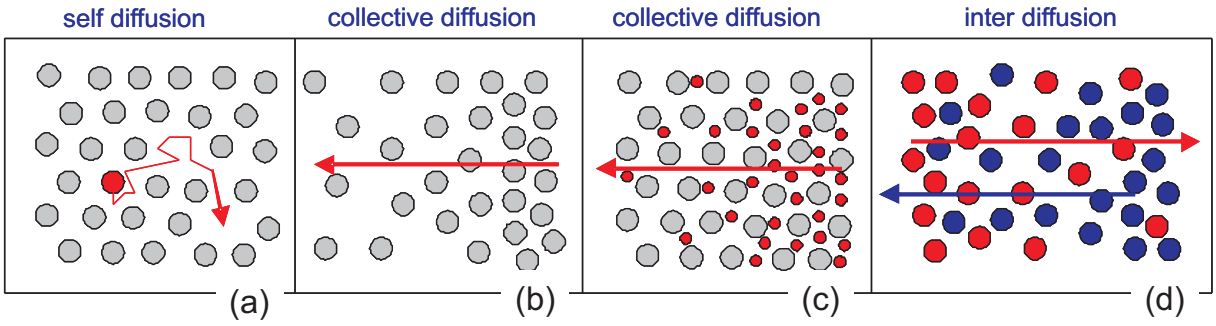

Fig. 1: *The three types of diffusion processes. (a) "self diffusion": the thermal motion of a single molecule, here for molecule within a crystalline solid with open interstitial positions. (b) "collective diffusion": a concentration gradient in a solution of molecules induced diffusive mass transport from the region of high concentration to the region of low concentration (as indicated by the arrow. (c) again collective diffusion, but now of small molecules (in red) through an essentially static environment of a crystalline solid. (d) "Inter diffusion": two different molecules (in blue and red), with opposite concentration gradients, mix due to diffusion. The arrows indicate the direction of net mass transport of the two components.*

same direction. This diffusion process is referred to as **inter diffusion**, and is depicted in Fig.1d, where the directions of the mass fluxes are indicated by the arrows.

Within the general classification of diffusion processes in self-, collective, and inter-diffusion, there is a great variety of different types of diffusion mechanisms for various types of systems. Some of these will be discussed quantitatively, and some only on a qualitative level. In this chapter we will focus on self- and collective-diffusion. Inter-diffusion will not be discussed.

Diffusive mass transport in stable systems is from regions of high concentration to low concentration. For thermodynamically unstable systems, however, strong attractive forces between molecules favor increase of concentration, where molecules are on average in each other's vicinity. The energy is lowered by increasing the concentration in part of the system due to the strong attractive interactions. Diffusion is now "uphill", from regions of low concentration to high concentration. Inhomogeneities thus increase in time, which is a kinetic stage during phase separation. The end-state is a coexistence between two phases. The initial stage of phase separation from an initially homogeneous, unstable system is discussed in section 4.

2 Self Diffusion

In this section we shall first develop a simple model in one dimension, where a molecule resides on discrete positions and can jump between these positions with a certain prescribed probability. In subsection 2.2 the discrete model will be cast in a continuum description, which allows for the explicit analysis of the time evolution of the probability density function for the position coordinate of a diffusing molecule. In subsection 2.3, the diffusion of a molecule in a periodic energy landscape will be analyzed, and compared to experiments. Finally, in subsection 2.4 a few other types of self-diffusion processes will be addressed on a qualitative level.

2.1 A simple model

As a first approach towards the understanding of diffusion processes, consider a single molecule that moves in one dimension and resides on discrete positions, as sketched in Fig.2. The distance between the discrete positions of the molecule is l, say, and the molecule is assumed to be at the site located at the origin at time $t=0$. The sites are indexed,

$$\{\cdots, -(n+1), -n, \cdots, -2, -1, 0, 1, 2, \cdots, n, (n+1), \cdots\} ,$$

where the "0" is the origin. The probability per unit time to make a "jump" to the left and right will be denoted by q and p, respectively. In the introduction we discussed self diffusion in case these two transition probabilities are equal. Taking $p \neq q$ is a generalization which can be thought of as self diffusion in an external force field, which induces a net average velocity of the molecule in the direction of the largest transition probability. We will come back to the effect of an external field at the end of this section.
Since diffusion is due to random thermal displacements, any theory that describes diffusion processes must be formulated in terms of probabilities. The probability to find the molecule at site n at time t will be denoted as $P(n,t)$. Since the probability to find the molecule at some site is unity, $P(n,t)$ is *normalized* in the sense that,

$$\sum_{n=-\infty}^{\infty} P(n,t) \;=\; 1 \; . \tag{2}$$

Since the molecule is supposed to be located at the origin at time zero, the probability for $n=0$ is unity at that time, while it is zero for all other n's,

$$P(n, t=0) \;=\; \delta_{n\,0} \; , \tag{3}$$

where the *Kronecker delta* $\delta_{n\,0}$ is unity for $n=0$ and zero for $n \neq 0$. For any function $f(n)$, its average value $< f > (t)$ at time t is equal to,

$$< f > (t) \;=\; \sum_{n=-\infty}^{\infty} f(n)\, P(n,t) \; . \tag{4}$$

An explicit expression for the probability $P(n,t)$ can in principle be found from the solution of its equation of motion, where the time derivative $\partial P(n,t)/\partial t$ is expressed in terms of $P(n,t)$. This so-called *master equation* can be constructed as follows. There is an increase of the probability to find the molecule at site n due to displacements from the neighbouring site $n-1$ to site n. The increase of $P(n,t)$ per unit time is equal to the probability $P(n-1,t)$ that the molecule is located at site $n-1$, multiplied by the transition rate p for the molecule to diffuse to the right. Similarly the increase of $P(n,t)$ per unit time due to jumps from site $n+1$ to the left is equal to $q\,P(n+1,t)$. There is a decrease of $P(n,t)$ due to jumps from site n to the neighbouring sites. This decrease per unit time is similarly equal to $(p+q)\,P(n,t)$. We thus arrive at the following master equation,

$$\frac{\partial}{\partial t} P(n,t) \;=\; p\,P(n-1,t) + q\,P(n+1,t) - (p+q)\,P(n,t) \; . \tag{5}$$

In principle this equation can be solved for $P(n,t)$, which then allows for the explicit calculation of averages (see eq.(4)).

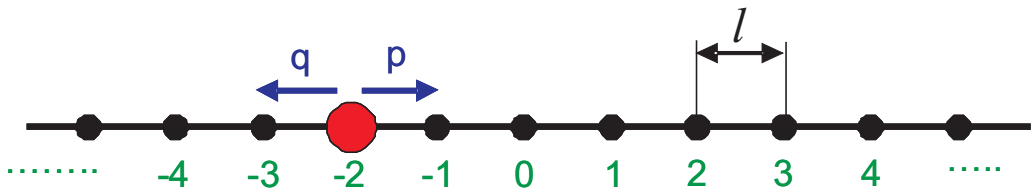

Fig. 2: *A molecule (indicated in red) diffusing in one dimension, which resides on lattice sites which are a distance l apart. At time zero the molecule is at the origin (the site with index 0). The transition rate for a displacement to the left is q, and to the right p.*

Of particular interest for self diffusion is the mean-squared displacement defined in eq.(1). In the extension to the case where $p \neq q$, as discussed above, there is an additional average that is related to the field-induced net displacement of the molecule, which we will refer to as the *drift velocity*. Let us first consider the average net velocity $<v>$ of the molecule, which is equal to,

$$<v> = l \frac{d}{dt} <n> (t) = l \sum_{n=-\infty}^{\infty} n \frac{\partial}{\partial t} P(n,t) . \tag{6}$$

Multiplying both sides of eq.(5) with n and summation over all n's leads to,

$$\frac{d}{dt} <n> (t) = \sum_{n=-\infty}^{\infty} n \left\{ p\, P(n-1,t) + q\, P(n+1,t) - (p+q)\, P(n,t) \right\} . \tag{7}$$

Each of the sums on the right hand-side can be explicitly evaluated. Consider as an example the first sum, which can be written as,

$$\sum_{n=-\infty}^{\infty} n\, P(n-1,t) = \sum_{m=-\infty}^{\infty} (m+1)\, P(m,t) = <n> (t) + 1 , \tag{8}$$

where the normalization identity (2) has been used. The remaining two sums can be evaluated similarly, leading to,

$$<v> = l \left\{ p - q \right\} . \tag{9}$$

Note that in case $p = q$, the drift velocity is zero, as it should. Next consider the mean-squared displacement. Multiplying both sides of the master equation (5) with n^2 and summing over all n's, it is found that.

$$\frac{d}{dt} W(t) = l^2 \sum_{n=-\infty}^{\infty} n^2 \left\{ p\, P(n-1,t) + q\, P(n+1,t) - (p+q)\, P(n,t) \right\} . \tag{10}$$

Similarly to the identity (8), the first sum can be written as,

$$\sum_{n=-\infty}^{\infty} n^2 P(n-1,t) = \sum_{m=-\infty}^{\infty} \left(m^2 + 2\,m + 1 \right) P(m,t) = <n^2> (t) + 2 <n> (t) + 1 , \tag{11}$$

and similarly for the two other contributions. This gives,

$$\frac{d}{dt} W(t) = l^2 \left(p + q \right) + 2\, l^2 \left(p - q \right)^2 t , \tag{12}$$

where it is used that $< n > (t) = l\,(p-q)\,t$, which follows from eq.(9) for the drift velocity. Integration with respect to time, and noting that $W(t=0)=0$ thus gives,

$$W(t) \;=\; l^2\;(\,p+q\,)\;t + l^2\;(\,p-q\,)^2\;t^2\;. \tag{13}$$

For pure diffusive motion where $p=q$, the mean-squared displacement therefore varies linearly with time. Typical distances $\sqrt{W(t)}$ over which a molecule diffuses during a time t thus vary like $\sqrt{t}$. Such a time dependence is typical for diffusive processes. The contribution $\sim t^2$ to the mean squared displacement in eq.(13) originates from the constant drift velocity. Note that the mean squared displacement $W_v(t)$ in a reference frame that moves along with the drift velocity is equal to,

$$W_v(t) \;\equiv\; l^2 < (\,n - < v > t\,)\;(\,n - < v > t\,) > = \; l^2\,(\,p+q\,)\;t\;, \tag{14}$$

which is the mean squared displacement for equal p and q.
A simple model for the difference between p and q due to an external field is most easily illustrated by considering a charged molecule in an external electric field. In an equilibrium system, the difference in the Boltzmann probability to find the molecule at two neighbouring sites is proportional to $\exp\{-\beta\,Q\,E\;l\}$, where $\beta = 1/k_BT$ (with k_B Boltzmann's constant, T the temperature), Q the charge carried by the molecule and E the electric field strength. This suggest the following form for the transition probabilities,

$$\begin{aligned} p &= \alpha\,\exp\left\{+\tfrac{1}{2}\,\beta\,Q\,E\,l\right\}\;, \\ q &= \alpha\,\exp\left\{-\tfrac{1}{2}\,\beta\,Q\,E\,l\right\}\;, \end{aligned} \tag{15}$$

where the electric field is chosen in positive direction, towards increasing index numbers. The prefactor α is the value of p and q in the absence of the field. For sufficiently small electric field strengths, where the Boltzmann exponents can be expanded to linear order in the electric field, it is thus found from eq.(9) that,

$$< v > = \;\frac{1}{\gamma}\;F\;, \tag{16}$$

where $F = Q\,E$ is the force exerted by the field on the charged molecule, and $\gamma = k_BT/\alpha\,l^2$ is a "*friction coefficient*". In the stationary state, where the drift velocity is constant, independent of time, the total average force on the molecule is zero. That is, the force on the molecule arising from "friction" with the surrounding matter must be equal to F in magnitude, but is opposite in sign. The friction force F_{fr} of the molecule with its surroundings is thus proportional to its velocity: $F_{fr} = -\,\gamma\,< v >$. The mean squared displacement, relative to the co-moving frame follows from eq.(14) as,

$$W_v(t) \;=\; 2\,D_s\,t\;, \tag{17}$$

where the **self diffusion coefficient** D_s is equal to,

$$D_s \;=\; \frac{k_B\,T}{\gamma}\;. \tag{18}$$

Since W_v is equal to the mean squared displacement in the absence of the field, this relation connects diffusive properties to the friction coefficient. This opens a way to calculate the self diffusion coefficient through the calculation of the friction coefficient. The relation (18) has been put forward by Einstein, and is therefore commonly referred to as the *Einstein relation*. This relation is generally valid, not just within the realm of the present simple model, as will be discussed later.

2.2 A continuum description

The master equation (5) can be cast into a differential equation, taking the limit where the distance l between the sites tends to zero. We consider here the case where the two transition probabilities p and q are both equal to α, say. To take the continuum limit, the master equation is rewritten as,

$$\frac{\partial}{\partial t} P(n,t) \;=\; \alpha\, l^2\, \frac{1}{l} \left[\frac{P(n+1,t) - P(n,t)}{l} - \frac{P(n,t) - P(n-1,t)}{l} \right] . \tag{19}$$

Each of the terms between the brackets is a first order spatial derivative with respect to position in the limit that $l \to 0$, so that the entire combination is a second order derivative. Replacing n by the continuously varying position x, it follows that,

$$\frac{\partial}{\partial t} P(x,t) \;=\; D_s \frac{d^2}{dx^2} P(x,t) \; , \tag{20}$$

where $D_s = \alpha\, l^2 = k_B T/\gamma$ is the self diffusion coefficient that was already introduced in the previous subsection. This equation of motion is easily extended to three dimensions, assuming that thermal displacements in the different Cartesian directions are independent, and the diffusion coefficient is the same for the three dimensions,

$$\frac{\partial}{\partial t} P(\mathbf{r},t) \;=\; D_s \left[\frac{\partial^2}{\partial x^2} + \frac{\partial^2}{\partial y^2} + \frac{\partial^2}{\partial z^2} \right] P(\mathbf{r},t) \equiv D_s\, \nabla^2\, P(\mathbf{r},t) \; . \tag{21}$$

Here $\mathbf{r} = (x,y,z)$ is the position coordinate of the molecule in three-dimensional space. Equations of motion of this sort are commonly referred to as **diffusion equations**, of which more general forms will be discussed later.
Contrary to the discrete case, where $P(n,t)$ is the probability to find the diffusing molecule at site n, the probability to find the molecule at a given position $\mathbf{r}$ with infinite accuracy is zero. In the continuum limit we have to work with so-called *probability density functions* (pdf's). The above pdf $P(\mathbf{r},t)$ is to be understood as follows,

> $P(\mathbf{r},t)\, d\mathbf{r}$ is the probability to find the molecule at time t with its center of mass within the infinitesimally small volume element $d\mathbf{r} = dx\, dy\, dz$ that is located at $\mathbf{r}$.

The continuum analogue of a thermal average for a discrete variable in eq.(4) is now a sum over all infinitesimally small boxes, that is,

$$< f > (t) \;=\; \int d\mathbf{r}\; f(\mathbf{r})\; P(\mathbf{r},t) \; , \tag{22}$$

for any (well-behaved) function f. Similar to the previous subsection, the mean squared displacement can be calculated without having to solve the diffusion equation. Taking, without loss of generality, the molecule at the origin at time $t = 0$, the mean squared displacement is equal to (see eq.(1)),

$$W(t) \;=\; \int d\mathbf{r}\; r^2\, P(\mathbf{r},t) \; . \tag{23}$$

Multiplying both sides of the diffusion equation with r^2 and integration leads to,

$$\frac{d}{dt} W(t) \;=\; D_s \int d\mathbf{r}\; r^2\, \nabla^2 P(\mathbf{r},t) \;=\; D_s \int d\mathbf{r}\; P(\mathbf{r},t)\, \underbrace{\nabla^2 r^2}_{=6} \;=\; 6\, D_s \; . \tag{24}$$

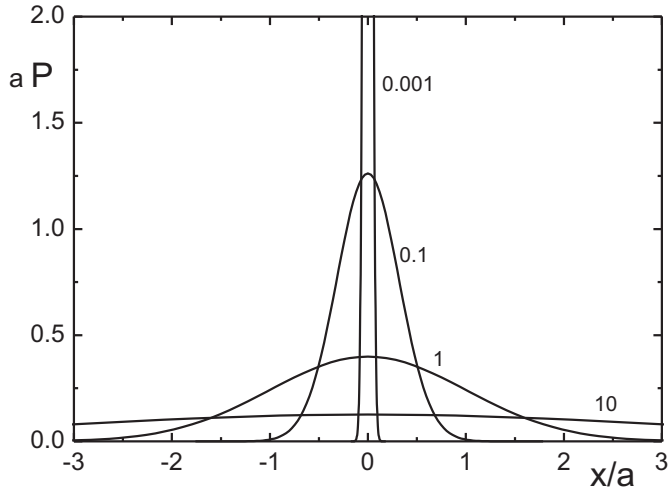

Fig. 3: *The probability density function $P(x,t)$ in eq.(27) (multiplied by the radius a of the spheres, as a function of x/a (with x the x-component of the position coordinate), for several values of the dimensionless time $\tau = t/\tau_a$, with $\tau_a = a^2/2\,D_s$ (the time required to reach a mean squared displacement in one direction equal to a^2), as indicated in the figure.*

In the second equation Green's second integral theorem is applied, and in the last line the continuum analogue of the normalization condition (2) is used. Note that each dimension contributes a $2D_s$. Since $W(t=0) = 0$ it follows that,

$$W(t) \;=\; 6\,D_s\,t\;, \tag{25}$$

in accordance with the result (17) for the mean square displacement in one dimension.
The initial condition that the molecule is at the origin at time $t = 0$ is mathematically formulated as,

$$P(\mathbf{r}, t=0) \;=\; \delta(\mathbf{r})\;, \tag{26}$$

where $\delta(\mathbf{r})$ is the *delta distribution*. This is the continuum analogue of the initial condition (3) for the discrete model. Imposing the above initial condition, the diffusion equation (21) can be solved analytically (with $r = |\,\mathbf{r}\,|$),

$$P(\mathbf{r},t) \;=\; \frac{1}{[\,4\,\pi\,D_s\,t\,]^{3/2}}\,\exp\left\{-\,\frac{r^2}{4\,D_s\,t}\right\}\;. \tag{27}$$

This function can be written as a product of the pdf for the x-, y- and z-coordinate, where the pdf for the x-coordinate is equal to,

$$P(x,t) \;=\; \frac{1}{[\,4\,\pi\,D_s\,t\,]^{1/2}}\,\exp\left\{-\,\frac{x^2}{4\,D_s\,t}\right\}\;, \tag{28}$$

and similarly for the y- and z-coordinates. This is a Gaussian pdf with a width that increases with time, as depicted in Fig.3. For short times the pdf is very sharply peaked (and ultimately

approaches the delta distribution as $t \rightarrow 0$), while for larger times the probability for large distances increases due to the diffusive displacement of the tracer molecule.
The equation of motion (21) can be generalized to include an external force acting on the molecule. First notice that the probability $P(\mathbf{r},t)$ can in principle be measured as follows. A molecule that resides at the origin is released at time zero, after which its trajectory is recorded. This experiment is repeated many times. In each of the experiments, the molecule follows a different trajectory. The number of trajectories that intersect, at time t, a small box centered at $\mathbf{r}$ measures the pdf $P(\mathbf{r},t)$. Alternatively, many non-interacting molecules can be released simultaneously, and each of the trajectories is recorded. Since the molecules do not interact with each other, they diffuse after release at time zero as if they were alone in the system. Each of the molecules thus exhibit self diffusion as described above. Again, the number of trajectories that intersect a small box at $\mathbf{r}$ after a time t measures the pdf $P(\mathbf{r},t)$. That number of trajectories, however, is also proportional to the local concentration $\rho_0(\mathbf{r},t)$ that one would measure (where the index "0" refers to non-interacting molecules). We can thus interpret $P(\mathbf{r},t)$ as the concentration $\rho_0(\mathbf{r},t)$ that exists when many non-interacting molecules are released at the origin $\mathbf{r}=\mathbf{0}$ at time $t=0$. The number density obeys the exact continuity equation,

$$\frac{\partial}{\partial t}\,\rho_0(\mathbf{r},t) \;=\; -\,\nabla\cdot\left[\,\rho_0(\mathbf{r},t)\,\mathbf{v}(\mathbf{r},t)\,\right]\;, \tag{29}$$

where $\mathbf{v}(\mathbf{r},t)$ is the thermally averaged velocity of molecules. When inertial forces are neglected (we shall comment on this at the end of this section), according to Newton's equation of motion, there is a balance of forces, that is, all non-inertial forces add up to zero. There are three forces to be considered. First of all there is the friction force $\mathbf{F}^{fr}=-\gamma\,\mathbf{v}$ that arises from interactions of the molecule with surrounding matter, where γ is the friction coefficient that was already introduced at the end of subsection 2.1. The second force is responsible for the velocity that the molecule attains in the absence of an external force field, and is referred to as the **Brownian force** $\mathbf{F}^{Br}$. The third force $\mathbf{F}^{ext}$ is due to an external field. By force balance we have,

$$\mathbf{F}^{fr}+\mathbf{F}^{Br}+\mathbf{F}^{ext} \;=\; \mathbf{0} \qquad\rightarrow\qquad \mathbf{v} \;=\; \frac{1}{\gamma}\,\left[\,\mathbf{F}^{Br}+\mathbf{F}^{ext}\,\right]\;. \tag{30}$$

Substitution into eq.(29) and comparing with eq.(21), with P replaced by ρ_0, in the absence of an external field, leads to $\mathbf{F}^{Br}=-\gamma D_s\,\nabla\ln\{\,\rho_0(\mathbf{r},t)\,\}$. For a conservative force field, for which $\mathbf{F}^{ext}=-\nabla\Phi$ (with Φ the external potential), and in case equilibrium is reached, the density must be proportional to the Boltzmann exponential $\rho_0\sim\exp\{-\Phi/k_BT\}$. On the other hand $\mathbf{v}=\mathbf{0}$ in equilibrium, which immediately leads to $\gamma\,D_s\,\nabla\ln\{\rho_0\}+\nabla\Phi=\mathbf{0}$, and hence, $\rho_0\sim\exp\{-\Phi/\gamma\,D_s\}$. It follows that $D_s=k_BT/\gamma$, which reproduces the Einstein relation (18) that we found within the simple model considered in subsection 2.1. It also follows that the Brownian force is equal to,

$$\mathbf{F}^{Br}(\mathbf{r},t) \;=\; -k_B\,T\,\nabla\,\ln\{\rho_0(\mathbf{r},t)\}\;, \tag{31}$$

with ρ_0 replaced by $P(\mathbf{r},t)$ when used in the equation of motion for the pdf $P(\mathbf{r},t)$. Using this expression for the Brownian force in eq.(29), and replacing the density ρ_0 by the pdf $P(\mathbf{r},t)$ thus leads to the generalization of the equation of motion eq.(21) to include an external force field,

$$\frac{\partial}{\partial t}\,P(\mathbf{r},t) \;=\; D_s\,\nabla\cdot\left[\,\nabla P(\mathbf{r},t)-\beta\,P(\mathbf{r},t)\,\mathbf{F}^{ext}(\mathbf{r})\,\right]\;. \tag{32}$$

We will use this equation in the next subsection to calculate the self diffusion coefficient of a molecule in a prescribed energy landscape.
In the above we assumed that inertial forces can be neglected. This is allowed on a time scale where the thermally averaged momentum coordinate, with a given initial value, relaxes to zero. According to Newton's equation of motion, without an external field,

$$\frac{d\,\mathbf{p}(t)}{dt} \;=\; -\frac{\gamma}{m}\,\mathbf{p}(t)\;, \tag{33}$$

where $\mathbf{p} = m\,\mathbf{v}$ is the momentum coordinate and m is the mass of the molecule. It follows that (with $\mathbf{p}_0$ the initial momentum at time zero),

$$\mathbf{p}(t) \;=\; \mathbf{p}_0\;\exp\{-t/\tau\} \quad , \quad \tau \;=\; m/\gamma\;. \tag{34}$$

The time scale τ on which the momentum coordinate relaxes is very typically much smaller than the time during which appreciable diffusion occurs, which validates the neglect of inertia. The time scale on which inertial forces can be neglected is commonly referred to as the **diffusive time scale**, while the dynamics on this time scale is referred to as **overdamped dynamics**. "overdamped" refers to the fact that friction forces are much larger than inertial forces.

2.3 Diffusion through a one-dimensional periodic energy landscape

As an example of an explicit calculation of the self diffusion coefficient we consider a molecule that interacts with its surroundings as described by a potential energy Φ. This potential is assumed to be periodic in one dimension, say the z-direction, and is constant along the other two directions : $\Phi \equiv \Phi(z)$. An experimental example that will be discussed at the end of this section is a rod-like molecule in a smectic phase that diffuses from one smectic layer to the other. The potential is assumed to be periodic with a period l, that is, $\Phi(z) = \Phi(z + n\,l)$ for any integer n. We shall calculate the friction coefficient γ and employ the Einstein relation $D_s = k_B T/\gamma$ to obtain the self diffusion coefficient in terms of the potential. In addition to the force $-\nabla\Phi$ due to interactions with the surroundings, there is thus an additional applied constant force F^{app} in the z-direction on the molecule that leads to a finite thermally averaged velocity.
For short times, the molecule "rattles within potential valleys". For longer times the molecule moves from one valley to the other, that is, it moves across potential barriers. On can therefore distinguish between a **short-time self-diffusion coefficient** that describes the thermal motion within a potential valley in the z-direction, and the **long-time self diffusion coefficient** that describes thermal displacements between valleys. Here we calculate the long-time self diffusion coefficient, which is relevant to mass transport on larger length scales.
The long-time self diffusion coefficient can be calculated from an eigen-function expansion of the solution of the diffusion equation (32), with $\mathbf{F}^{ext} \equiv -\nabla\Phi + \mathbf{F}^{app}$ [1]. Alternatively, an expression for the long-time self diffusion coefficient can be obtained without having to solve the diffusion equation explicitly [2]. First of all, we identify the pdf $P(x,t)$ as the concentration of non-interacting molecules, an identification that has been discussed in subsection 2.2. Instead of analyzing the motion of a single molecule under the action of the force $\mathbf{F}^{app}$, one can analyze the motion of many non-interacting molecules simultaneously. Since the molecules do not interact with each other, they move as if they were alone in the system, and hence they all move like a self-diffuser. The stationary flux j_0 of molecules in the x-direction is equal to (the indices

"0" refer to "non-interacting molecules"),

$$j_0 \;=\; \rho_0(z)\, v(z) \;=\; \bar{\rho}\, \exp\{-\beta\, \Phi(z)\}\; v(z)\;, \tag{35}$$

where $\bar{\rho}$ is the number density that would have existed in the absence of the potential. This expression is valid up to order $(F^{app})^2$. The velocity is linear in F^{app}, so that the zeroth-order solution for $\rho_0 \equiv P$ of eq.(32) with $\mathbf{F}^{ext} \equiv -\nabla\Phi$ can be used.
Let τ be the mean time spend by a molecule within a valley. The mean velocity $\bar{v}$ can then be expressed as (again, l is the periodicity of the potential),

$$\bar{v} \;=\; l/\tau\;. \tag{36}$$

The number of molecules N_u within a single valley over an area $A_\perp$ in the yz-plane is equal to,

$$N_u/A_\perp \;=\; j_0\,\tau \;=\; \int_{-l/2}^{l/2} dz\; \rho_0(z) \;=\; l\,\bar{\rho}\;\prec \exp\{-\beta\,\Phi\}\succ\;, \tag{37}$$

where the brackets define the periodicity average,

$$\prec f \succ \equiv\; \frac{1}{l}\int_{-l/2}^{l/2} dz\; f(z)\;, \tag{38}$$

for any function $f(z)$. The last step in eq.(37) is valid up to leading order in F^{app}. Note that j_0 is linear in F^{app}, while τ varies like $1/F^{app}$ for sufficiently small applied forces, so that their product is a constant to leading order.
The force balance relation (30) for the present case reads,

$$F^{fr} + F^{app} - \frac{d}{dz}\,\{\, k_B T \ln\rho_0 + \Phi\,\} \;=\; 0\;. \tag{39}$$

The local friction force F^{fr} is equal to $-\gamma_0\, v(z)$, where γ_0 is the friction coefficient in the absence of the potential Φ. On integration of both sides from $z = -l/2$ to $+l/2$, the gradient contribution vanishes due to symmetry, and hence,

$$F^{app} \;=\; \gamma_0\,\frac{1}{l}\int_{-l/2}^{l/2} dz\; v(z)\;. \tag{40}$$

Combining the above equations we have,

$$\begin{aligned}
\frac{1}{l}\int_{-l/2}^{l/2} dz\; v(z) \;&\underbrace{=}_{eq.(35)}\; \frac{j_0}{\bar{\rho}}\;\prec \exp\{+\beta\Phi\}\succ \\
&\underbrace{=}_{eq.(37)}\; \frac{l}{\tau}\;\prec \exp\{-\beta\Phi\}\succ \prec \exp\{+\beta\Phi\}\succ \\
&\underbrace{=}_{eq.(36)}\; \bar{v}\;\prec \exp\{-\beta\Phi\}\succ \prec \exp\{+\beta\Phi\}\succ\;.
\end{aligned} \tag{41}$$

Hence, by substitution into eq.(40),

$$F^{app} \;=\; \gamma\,\bar{v}\quad,\quad \text{with}\quad \gamma \;=\; \gamma_0\;\prec \exp\{-\beta\Phi\}\succ \prec \exp\{+\beta\Phi\}\succ\;. \tag{42}$$

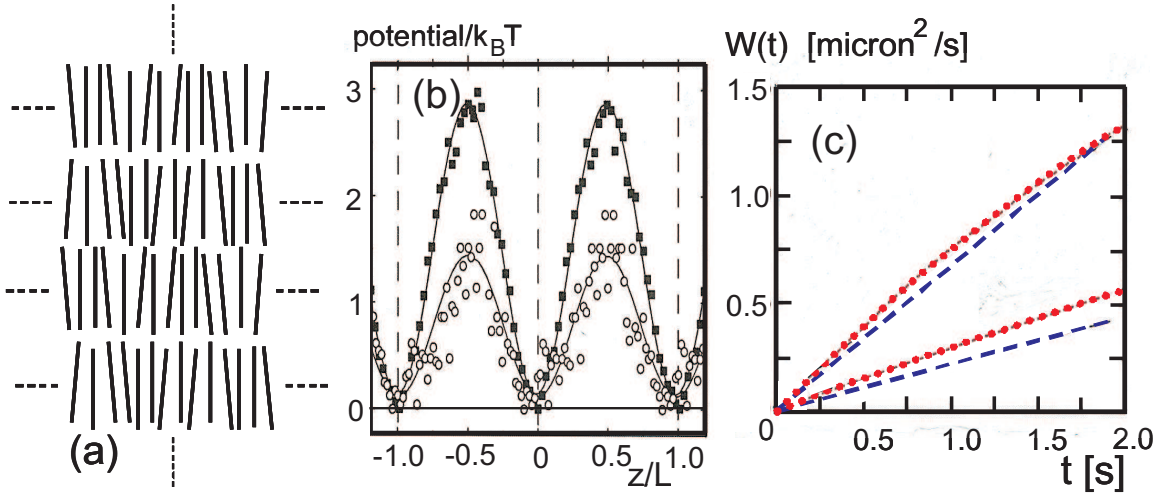

Fig. 4: *(a) A sketch of a smectic phase. (b) The potential that a given rod experiences due to interactions with surrounding rods. Two potentials are shown: the solid data points* ■ *are for an ionic strength of* $20\ mM$*, and the open symbols* ∘ *refer to an ionic strength of* $110\ mM$*. (c) Mean-squared displacements as a function of time for the two ionic strengths* 20 *(lower two curves) and* $110\ mM$ *(upper curves). The red dotted lines are experimental, and the blue dashed lines are obtained from eq.(43). Data are taken from Ref.[3].*

The long-time self diffusion coefficient D_s^l is thus found from the Einstein relation to be equal to,

$$D_s^l \;=\; \frac{D_s^0}{\prec \exp\{-\beta\Phi\} \succ \prec \exp\{+\beta\Phi\} \succ}\;, \tag{43}$$

where D_s^0 is the self diffusion coefficient in the absence of the potential Φ.
Diffusion of colloidal rod-like particles across smectic layers provides an experimental test of this relation [3, 4]. A smectic phase is spontaneously formed by systems of rod-like particles at sufficiently high concentration. This structure consists of a stack of mono-layers of rods with a preferred direction of alignment in the stacking direction, as sketched in Fig.4a. There is diffusion within the layers, and there is an exchange of rod-like particles between the layers. The long-time self diffusion coefficient corresponding to exchange between layers is given by eq.(43), where the potential is now set up by the interaction of the tracer rod with the surrounding rods. The assumption here is that the fluctuations of the position and width of the smectic layers can be neglected, so that the potential is a given function of the position of the tracer rod. This potential can be measured through the residence time of rods at prescribed positions. The residence time is inversely proportional to the probability $\sim \exp\{-\beta\,\Phi(z)\}$ to find a rod at position z (the direction perpendicular to the smectic planes). The experiments discussed here are performed with fd-virus particles in water. Fd-viruses are very long ($880\ nm$) and thin ($6.8\ nm$) stiff rods, consisting of a DNA strand which is rendered stiff by so-called coat-proteins that are attached to the DNA. The potential for this system, as obtained from residence times, is given in Fig.4b for two ionic strengths: 20 and $110\ mM$. The ionic strength changes the interactions between the rods and therefore the potential set up by the smectic layers. The solid line is a best fit to a sinusoidal function, which described the potential accurately. The long-time self diffusion coefficient can be measured independently by tracing rod-like colloids by means of time-resolved microscopy, where the tracer rod is fluorescently labeled while the

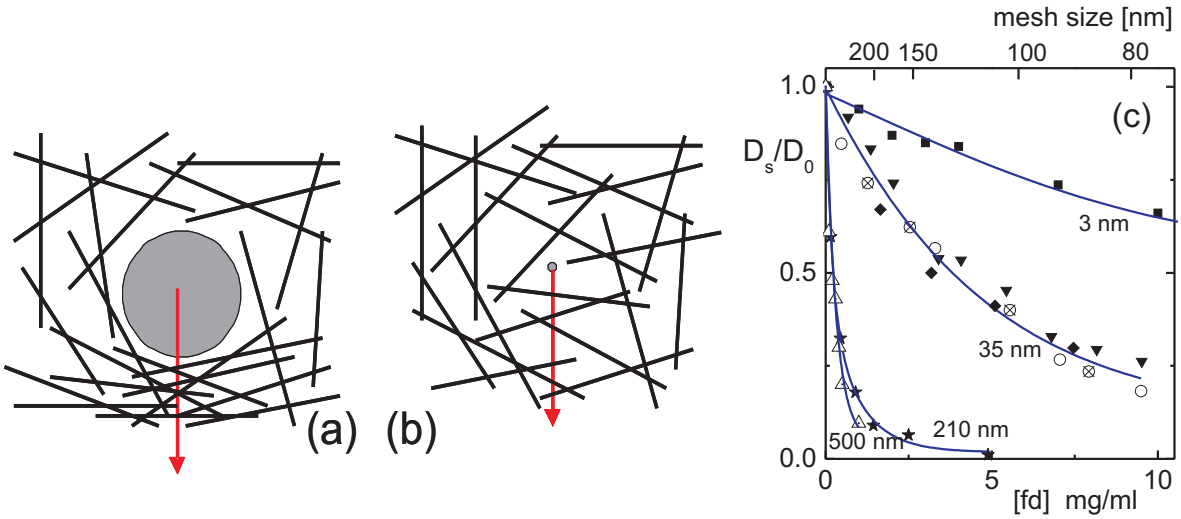

Fig. 5: *(a) Diffusion of a sphere through a rod-network, where the sphere is much large than the mesh size of the network. A displacement is accompanied by structural deformation of the network. Typically, rods accumulate in front of the sphere. (b) Diffusion of a small sphere, much smaller than the mesh size. The network structure is essentially unaffected by motion of the sphere, and hydrodynamic interactions with the network are dominant. (c) The long-time collective diffusion coefficient of spherical tracers of various sizes (as indicated) through fd-virus fiber networks as a function of fd-concentration (lower axis) and the mesh size of the network (upper axis). Various symbols of data points refer to different experimental techniques (particle tracking, fluorescence correlation spectroscopy and dynamic light scattering). This plot is taken from Ref.[6].*

remaining rods are not fluorescent. The resulting mean-squared displacement is given as a function of time in Fig.4c, for the two ionic strengths (the red dotted lines). The blue dashed lines in Fig.4c corresponds to the prediction (43) with the use of the potential given in Fig.4a. The slope of these lines line is twice the diffusion coefficient, since we are dealing here with diffusion in one dimension. The free diffusion coefficient D_s^0 is in this case the diffusion coefficient along the director in the nematic phase, just below the nematic-smectic phase transition concentration. The comparison of the experiments with the prediction in eq.(43) involves therefore no fitting parameters. The experimental upper curves deviate somewhat from straight lines, which is probably due to the transition from short-time diffusion to long-time diffusion. Quite detailed experiments on diffusion of spherical colloids through a sinusoidally varying energy landscape set up by an electric field can be found in Ref.[5].

2.4 Other self-diffusion processes

There are many other types of self-diffusion processes. A concise overview of all the self-diffusion processes and mechanisms is outside the scope of this chapter. In this subsection, we will discuss three other self-diffusion processes on a qualitative level.
Diffusion of spherical colloids through networks of very long and thin rods (or fibers) is another example where the friction coefficient is affected by interactions of the diffusion species (the

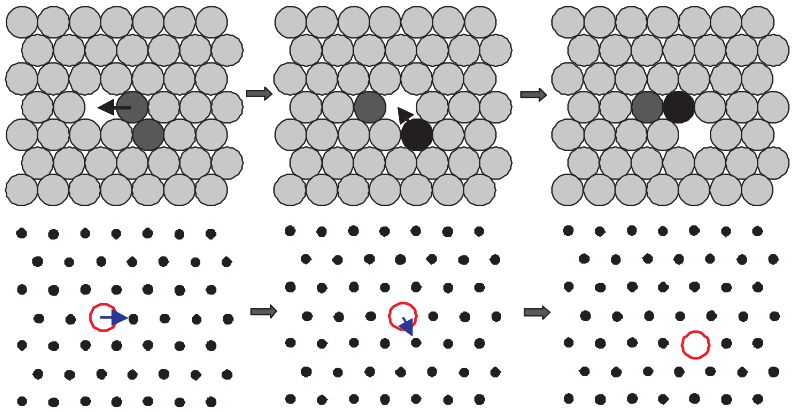

Fig. 6: *The mechanism of vacancy diffusion. In the upper three panels, the consecutive nearest neighbour displacement of the black-coloured molecules lead to motion of the vacancy, as shown schematically by the red circle in the lower panel.*

tracer sphere) and its surroundings (the rod-network). Such a self-diffusion process can not be described in terms of an external potential like for the above example in subsection 2.3. For this case the diffusion equation must be solved explicitly, which, again, is beyond the scope of this chapter. In case the tracer sphere sphere is much larger than the mesh size of the rod-network, the friction coefficient is mainly affected by the deformation of the network as the sphere is pulled through (see the sketch in Fig.5a). At first sight one might expect that diffusion of very small spheres, much smaller than the mesh size of the network (as sketched in Fig.5b) is essentially equal to the free diffusion diffusion coefficient, in the absence of the network. There is, however, an aspect that we have not discussed so far, which affects the friction coefficient even for these small tracer spheres. As the sphere moves through the solvent, it sets the solvent in motion. This fluid flow will be reflected by the network back to the sphere, which is thereby affected in its motion. These so-called **hydrodynamic interactions** contribute to the (long-time) friction coefficient, so that the diffusion coefficient is less than that of the freely diffusing sphere. For the large sphere, hydrodynamic interactions are relatively small as compared to direct interactions with the rods, while for small spheres, with a diameter that is of the order or smaller than the network mesh size, hydrodynamic interactions are dominant. Experimental data for long-time diffusion are given in Fig.5c, where the fiber network is formed by the same fd-virus particles as discussed in subsection 2.3 (which are $880\ nm$ long and $6.8\ nm$ thick, and relatively stiff). As can be seen, the effect of deformation of the network for the large spheres has a much more pronounced effect that hydrodynamic interactions for the smaller spheres. More details can be found in Refs.[6, 7, 8].

In crystals the position of single vacancies changes due to thermal motion of the surrounding molecules. The thermal displacement of a vacancy is the result of motion of neighbouring molecules to the actual vacancy position (as schematically shown in Fig.6). As the vacancy displacement is related to thermal motion of neighbouring molecules, vacancies obey the same diffusion laws as if it were a material-particle, and one can correspondingly define a **vacancy diffusion coefficient**. In order for the vacancy to move to a neighbouring position, the corresponding motion of a molecule that moves in the opposite direction requires it to move over an energy barrier (of height E, say) that is determined by the interactions with the remaining molecules in the crystal. Since the probability for a molecule to attain this energy is proportional to $\exp\{-\beta E\}$, the vacancy diffusion coefficient is also proportional to this exponent.

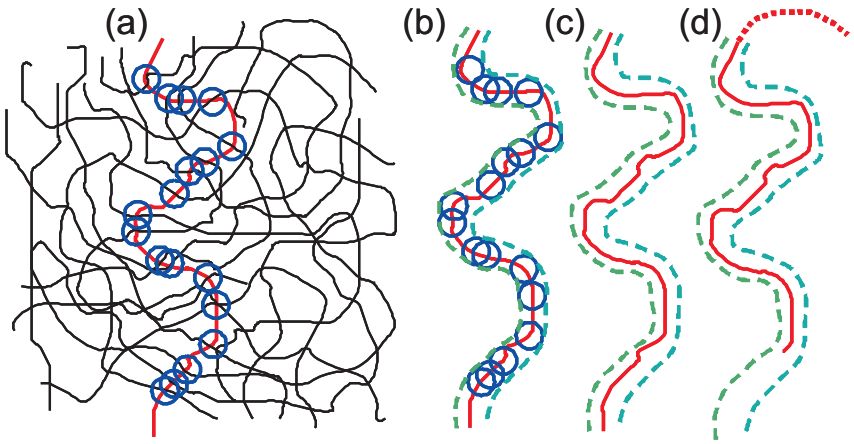

Fig. 7: *Reptation diffusion mechanism of flexible polymers. (a) a polymer chain (in red) within the matrix of other chains. The interaction points with other chains (indicated by circles in (b)) creates a "tube" as indicated in green in (c), through which the tagged chain can move out by diffusion, as depicted in (d).*

The same arguments hold for the diffusion of an interstitial atom through a crystal. Experimentally one therefore often finds that self diffusion coefficients exhibit a so-called **Arrhenius behaviour**, that is, the logarithm of the diffusion coefficient varies linearly with the reciprocal temperature $1/T$. The slope is equal to $-E/k_B$, from which the "**diffusion activation energy**" E is obtained.
So far only molecules of a spherical- and rod-like molecules have been discussed. Flexible molecules, like polymers, will of course also exhibit diffusion. Due to the high degree of entanglement in melts and solutions of polymers, single-polymer diffusive motion can be described by the so-called **tube model**. The interactions with neighbouring polymers (see Fig.7a) defines a "tube" within which a given polymer chain can diffuse (see Figs.7b,c). The given polymer chain can then find another tube after diffusion of one of the ends of the polymer chain outward the original tube (see Fig.7d) [9, 10, 11]. This **reptation mechanism** has been extended to include, for example, the dynamics of the tube itself and the retraction of the polymer within the tube.

3 Collective Diffusion

Contrary to self diffusion, collective diffusion describes the net mass transport due to gradients in concentration, as already discussed in the introduction. Similar to self diffusion, the first step towards a theory to describe diffusive mass transport is to derive an equation of motion for the concentration of the diffusing species. A simple diffusion equation has been proposed by Fick more than a century ago. The assumption he made is that the mass flux $\mathbf{j}$ of molecules is linear in concentrations gradients, that is,

$$\mathbf{j}(\mathbf{r},t) \;=\; -D_c\,\nabla\rho(\mathbf{r},t)\;, \tag{44}$$

provided that concentration gradients are sufficiently small. Here $\rho(\mathbf{r},t)$ is the instantaneous number density (number of molecules per unit volume) at position $\mathbf{r}$ and time t. Furthermore, the proportionality constant D_c is referred to as the **collective diffusion coefficient**, and $\nabla =$

$(\partial/\partial x, \partial/\partial y, \partial/\partial z)$ is the nabla- or gradient-operator. A minus sign is added to the right hand-side in eq.(44) to render D_c positive (note that the flux is typically directed towards regions of low concentration, as already discussed in the introduction). Substitution of this expression for the flux into the continuity equation gives,

$$\frac{\partial}{\partial t}\,\rho(\mathbf{r},t) \;=\; -\nabla\cdot\mathbf{j}(\mathbf{r},t) \;=\; \nabla\cdot\left[\,D_c\,\nabla\,\rho(\mathbf{r},t)\,\right]\;. \tag{45}$$

In concentrated systems, the collective diffusion coefficient depends on concentration, $D_c \equiv D_c(\rho(\mathbf{r},t))$, so that it can not placed in front of the $\nabla-$ operator. Suppose, however, that the deviation of the density from its average value is small. That is, $\rho(\mathbf{r},t) = \bar{\rho} + \delta\rho(\mathbf{r},t)$, with $\delta\rho(\mathbf{r},t)/\bar{\rho} \ll 1$, where $\bar{\rho}$ is the number density of the system without concentration gradients. When this is assumed, the diffusion equation (45) can be written, up to linear order in $\delta\rho(\mathbf{r},t)$, as,

$$\frac{\partial\rho(\mathbf{r},t)}{\partial t} \;=\; D_c\,\nabla^2\rho(\mathbf{r},t)\;, \tag{46}$$

The assumption of small overall deviations from the average density is a quite severe assumption that is not satisfied for many cases, so that eq.(45) is relevant rather than eq.(46). For very dilute systems, where inter-molecular interactions are absent, this is a valid procedure, since then D_c is indeed a constant. In that case eq(46) reproduces eq.(21) for self diffusion (as discussed in subsection 2.2, this equation also holds for the concentration when interactions between the tracer molecules are absent). It follows that, for very dilute system, the self- and collective diffusion coefficients are identical,

$$D_s^0 \;=\; D_c^0\;, \tag{47}$$

where the superscript "0" is used to indicate that interactions between diffusing species are absent. In most practical systems, the concentration of diffusing molecules is large, such that inter-molecular interactions are important for the diffusive properties. The collective diffusion coefficient under such conditions is different from D_c^0, and depends on the interactions between molecules. We will therefore extend the diffusion equation for infinite dilution to include inter-molecular interactions in subsection 3.1. In subsection 3.2, **Fick's law** (45) will be derived from this generalized diffusion equation, and an explicit expression will be obtained for the collective diffusion coefficient in terms of the interaction potential between the molecules. The specific example of diffusion of hydrogen through metal crystals is then discussed in subsection 3.3.
One possible way to think about the physical meaning of the collective diffusion is as follows. Suppose that at time $t = 0$ there is a sinusoidal concentration profile, $\rho(\mathbf{r}, t=0) = \bar{\rho} + \Delta\rho_0 \times \sin\{\mathbf{k}\cdot\mathbf{r}\}$, where $\Delta\rho_0$ is the initial amplitude of the density variation superimposed on a constant overall concentration $\bar{\rho}$. The wavelength Λ of this sinusoidal density variation is equal to,

$$\Lambda \;=\; \frac{2\,\pi}{k}\;, \tag{48}$$

with k the length of the *wave vector* $\mathbf{k}$. Substitution of the Ansatz $\rho(\mathbf{r},t) = \bar{\rho} + \Delta\rho(t)\times\sin\{\mathbf{k}\cdot\mathbf{r}\}$ into Fick's diffusion equation (46) gives the time-dependent amplitude of the density variation equal to,

$$\Delta\rho(t) \;=\; \Delta\rho_0\,\exp\{-D_c\,k^2\,t\}\;. \tag{49}$$

The collective diffusion coefficient thus determines how fast a sinusoidal concentration profile relaxes. The relaxation rate varies with the wavelength as $\sim \Lambda^{-2}$, the interpretation of which is that it takes particles longer to diffuse over longer distances, while the time it takes to diffuse over a certain distance is quadratically depending on that distance (as quantified by eq.(25) for the mean-squared displacement of a single particle). As will be seen in the next subsection, the validity of eq.(46) (and hence of eq.(49)) is limited to wavelengths that are much larger than the range of the pair-interaction potential between the diffusing particles. When the pair-interactions between particles is repulsive, it is intuitively obvious that the particles in regions of high concentration are pushed apart more strongly at higher overall concentrations $\bar{\rho}$, which leads to a faster relaxation. In other words, the collective diffusion coefficient is expected to increase with increasing overall concentration. For the same reason a decrease is expected for particles with attractive pair-interaction potentials. The above intuitive arguments are only valid for sufficiently low concentrations $\bar{\rho}$, such that interactions between two given particles is not too much affected by the presence of other particles. At sufficiently high concentrations, the collective diffusion coefficient can decrease with increasing concentration $\bar{\rho}$ due to indirect interactions at large overall concentrations also for repulsive pair-interactions potentials. In addition to direct interactions, also hydrodynamic interactions can play an important role in the concentration dependence of the collective diffusion coefficient of particles in a solvent. A moving particle in a solvent induces a fluid flow that affects other particles in their motion, and therefore the value of the collective diffusion coefficient. Such hydrodynamic interactions will not be discussed in this chapter (more about the concentration dependence of diffusion coefficients of spherical particles in a solvent and hydrodynamic interactions can be found in, for example, Ref.[12, 13, 14]). While the collective diffusion coefficient increases with concentration in case of repulsive interactions, it is obvious that the self diffusion coefficient decreases. Due to the repulsive interactions with neighbouring particles, the diffusive displacement of a given particle is hindered, leading to a decrease of the mean-squared displacement, and thus to a smaller self diffusion coefficient.
Attractive interactions between particles can be so strong, that it is energetically favorable to increase an initial inhomogeneity. According to eq.(49) this happens when the collective diffusion coefficient is negative. A homogeneous system with a negative collective diffusion coefficient is unstable in the sense that arbitrary small fluctuations in the concentration leads to the formation of inhomogeneities. Such a growth of inhomogeneities, that ultimately leads complete phase separation, is referred to as **spinodal decomposition**. Spinodal decomposition will be discussed in some detail in section 4.

3.1 A generalized diffusion equation

As discussed at the end of subsection 2.2, there is force balance in the overdamped limit (or equivalently, on the diffusive time scale). Since inertial forces can be neglected, all other forces add up to zero on the diffusive time scale. In the dilute limit, where interactions between molecules can be neglected, force balance results in the expression (30) for the velocity of a given molecule, with the Brownian force being given in eq.(31) (where the number density is now denoted as ρ, without the subscript "0", since we here consider the more general case of concentrated systems). For interacting molecules, at relatively high concentration, the external force in eq.(30) is equal to the force that acts on a given molecule due to interactions with neighbouring molecules. We will denote this force by $\mathbf{F}^I$ instead of $\mathbf{F}^{ext}$, to indicate that the force is now due to inter-molecular interactions.

The force $\mathbf{F}^I$ on a molecule at $\mathbf{r}$ due to the presence of a second molecule at $\mathbf{r}'$ is equal to $-\nabla V(|\,\mathbf{r}-\mathbf{r}'\,|)$, with V the pair-interaction potential. The force experienced by the molecule at $\mathbf{r}$ is equal to this pair-force, multiplied by the number of neighbouring molecules around the give molecule at position $\mathbf{r}$, averaged over all positions $\mathbf{r}'$ of neighbouring molecules,

$$\mathbf{F}^I(\mathbf{r},t) \;=\; -\int d\mathbf{r}'\; g(\mathbf{r},\mathbf{r}',t)\,\rho(\mathbf{r}',t)\,\nabla V(|\,\mathbf{r}-\mathbf{r}'\,|)\;, \tag{50}$$

where $g(\mathbf{r},\mathbf{r}',t)$ is the probability to find a molecule at $\mathbf{r}'$, given that there is a molecule at $\mathbf{r}$. This **conditional probability density function** is commonly referred to as **the pair-correlation function**. From the above mentioned force balance, we have, $\gamma_0\,\mathbf{v} = \mathbf{F}^{Br} + \mathbf{F}^I$, where γ_0 is the friction coefficient at infinite dilution, that is, in the absence of inter-molecular interactions. The corresponding flux $\mathbf{j} = \rho\,\mathbf{v}$ is thus equal to,

$$\mathbf{j}(\mathbf{r},t) \;=\; -D_c^0\left[\nabla\rho(\mathbf{r},t) + \beta\,\rho(\mathbf{r},t)\int d\mathbf{r}'\; g(\mathbf{r},\mathbf{r}',t)\,\rho(\mathbf{r}',t)\,\nabla V(|\,\mathbf{r}-\mathbf{r}'\,|)\right]\;, \tag{51}$$

where, as before, $\beta = 1/k_BT$ and $D_c^0 = k_BT/\gamma_0$. This expression for the flux can be substituted into the exact conservation equation, to obtain a **generalized diffusion equation**,

$$\begin{aligned}\frac{\partial\rho(\mathbf{r},t)}{\partial t} \;&=\; -\nabla\cdot\mathbf{j}(\mathbf{r},t)\\ &=\; D_c^0\left[\nabla^2\rho(\mathbf{r},t) + \beta\,\nabla\cdot\left\{\rho(\mathbf{r},t)\int d\mathbf{r}'\; g(\mathbf{r},\mathbf{r}',t)\,\rho(\mathbf{r}',t)\,\nabla V(|\,\mathbf{r}-\mathbf{r}'\,|)\right\}\right]\;.\end{aligned} \tag{52}$$

This is the fundamental equation of motion that will be used in the sequel to analyze the collective diffusion at finite concentrations.

3.2 Derivation of Fick's law for concentrated systems

The generalized diffusion equation (52) can be used to derive Fick's law (45), where an explicit expression will be obtained for the collective diffusion coefficient D_c in terms of the pair-interaction potential V. The linear relationship (44) between the mass flux and spatial gradients in the concentration is expected to hold only for sufficiently small gradients. We will therefore assume that on the distance R_V over which the pair-potential V falls off to zero, the density is essentially a linear function of position. The following Taylor expansion can thus be used in the integral in eq.(52) (with $\mathbf{R} = \mathbf{r}^{'} - \mathbf{r}$,),

$$\rho(\mathbf{r}^{'},t) \;\approx\; \rho(\mathbf{r},t) + \mathbf{R}\cdot\nabla\rho(\mathbf{r},t)\;, \tag{53}$$

since the pair-potential limits the integration range in $\mathbf{r}^{'}$-space to a region of extent R_V around $\mathbf{r}$. Here the "$\cdot$" is the inner product of the two vectors on both sides. An appropriate approximation for the pair-correlation function can be obtained as follows. First of all, we need an approximation only for $|\,\mathbf{r}-\mathbf{r}^{'}\,| \leq R_V$. For such small, microscopic distances, the pair-correlation function relaxes essentially instantaneous to equilibrium relative to the time scale on which the concentration evolves. We can therefore take the pair-correlation function equal to its equilibrium value g^{eq}. This approximation can be considered as a statistical mechanical analogue of the **thermodynamic local equilibrium** assumption that is made in the theory of

irreversible thermodynamics. A natural choice is to take this equilibrium function equal to that of a homogenous system with a density in between the points $\mathbf{r}$ and $\mathbf{r}^{'}$,

$$g(\mathbf{r},\mathbf{r}^{'},t) \;\approx\; g^{eq}(|\,\mathbf{r}-\mathbf{r}^{'}\,|) \quad , \quad \rho \equiv \rho\left(\frac{\mathbf{r}+\mathbf{r}^{'}}{2},t\right) \; . \tag{54}$$

Note that due to translational and rotational invariance of a homogeneous system, the pair-correlation function depends on $\mathbf{r}$ and $\mathbf{r}^{'}$ only through $|\,\mathbf{r}-\mathbf{r}^{'}\,|$. Thus, again Tayloring up to linear spatial dependencies, after writing $(\mathbf{r}+\mathbf{r}^{'})/2$ as $\mathbf{r}+\frac{1}{2}\,\mathbf{R}$,

$$\begin{aligned} g(\mathbf{r},\mathbf{r}^{'},t) \;&\approx\; g^{eq}(R) + \left\{\,\rho\left(\frac{\mathbf{r}+\mathbf{r}^{'}}{2},t\right) - \rho(\mathbf{r},t)\,\right\}\,\frac{d}{d\rho}\,g^{eq}(R) \\ &\approx\; g^{eq}(R) + \tfrac{1}{2}\,\frac{dg^{eq}(R)}{d\rho}\,\mathbf{R}\cdot\nabla\rho(\mathbf{r},t) \;\; , \end{aligned} \tag{55}$$

where $g^{eq}(R,t)$ is the equilibrium pair-correlation function for a homogeneous system with concentration $\rho(\mathbf{r},t)$, which is thus an implicit function of $\mathbf{r}$ and t, and the density derivative is with respect to $\rho(\mathbf{r},t)$. This implicit dependence is not denoted here explicitly for brevity. Substitution of the expansions (53,55) into the integral in eq.(52), using that $\nabla V(|\,\mathbf{r}-\mathbf{r}^{'}\,|) = -\hat{\mathbf{R}}\,dV(R)/dR$ (with $\hat{\mathbf{R}}=\mathbf{R}/R$ the unit vector along $\mathbf{R}$), together with,

$$\begin{aligned} \oint d\hat{\mathbf{R}}\;\hat{\mathbf{R}} \;&=\; \mathbf{0}\;, \\ \oint d\hat{\mathbf{R}}\;\hat{\mathbf{R}}\,\hat{\mathbf{R}} \;&=\; \frac{4\pi}{3}\,\hat{\mathbf{I}}\;, \end{aligned} \tag{56}$$

where the integrals range over all directions of $\mathbf{R}$, and $\hat{\mathbf{I}}$ is the identity tensor, leads to,

$$\rho(\mathbf{r},t)\int d\mathbf{r}'\; g(\mathbf{r},\mathbf{r}',t)\,\rho(\mathbf{r}',t)\,\nabla V(|\,\mathbf{r}-\mathbf{r}'\,|) \;=\; \frac{2\pi}{3}\,\nabla\rho\,\frac{d}{d\rho}\left[\rho^2\int_0^\infty dR\;R^3\,\frac{dV(R)}{dR}\,g^{eq}(R)\right]. \tag{57}$$

We can now employ the standard equilibrium statistical mechanical expression for the pressure P^{eq},

$$P^{eq} \;=\; \rho\,k_BT - \frac{2\pi}{3}\,\rho^2\int_0^\infty dR\;R^3\,\frac{dV(R)}{dR}\,g^{eq}(R)\;, \tag{58}$$

to obtain Fick's diffusion equation (45) with,

$$D_c(\rho(\mathbf{r},t)) \;\equiv\; D_c^0\,\beta\,\frac{dP^{eq}(\rho(\mathbf{r},t))}{d\rho(\mathbf{r},t)}\;. \tag{59}$$

When gradients in concentrations are very large, such that the concentrations varies non-linearly on length scales set by the range R_V of the inter-molecular pair-potential, the Taylor expansions (53,55) are inaccurate, and higher orders of ∇ come into play in the diffusion equation.
Note that $(dP^{eq}/d\rho)\;\nabla\rho = \nabla P^{eq}$, which suggests that mass transport is driven by gradients in the pressure, which is intuitively appealing.
There is a subtlety for solutions of macromolecules. Instead of the mechanical pressure, the osmotic pressure appears in eq.(59) for the diffusion coefficient. This is a consequence of the fact that the macro-molecular pair-correlation function is thermally averaged with respect to the degrees of freedom of the solvent molecules. Furthermore, we neglected hydrodynamic interactions between such macromolecules, which do have an effect on the diffusive properties. A detailed discussion of these facts is beyond the scope of this chapter. The full expression for the diffusion coefficient of spherical macromolecules in solution, including the effects of hydrodynamic interactions, can be found in, for example, Ref.[12, 13, 14].

3.3 Diffusion of hydrogen through metals

Diffusion of hydrogen through metals has been studied since about 1850, and revived as a research area some decades ago due to the possible applications in energy storage. Hydrogen dissolves in metals not as intact H_2-molecules but as H-atoms, which reside at interstitial positions of the metal's crystal structure. There is a large number of neighbouring interstitial positions, so that hydrogen diffuses much faster as compared to diffusion of a molecule, where a thermal displacement requires the improbable event that there is a neighbouring vacancy (a missing atom in the crystal) to which it can move to. Fast diffusion of hydrogen is important for possible energy storage, since hydrogen must be dissolved in the metal (upon storage) and removed from the metal (upon use) within a reasonable time. Other important aspects for energy storage are the amount of hydrogen that can be dissolved, the effect of the mechanical properties of the metal on dissolving hydrogen, and the processes that occur right after absorption of hydrogen at the metal's surface, One of the metals in which large amounts of hydrogen can be dissolved is palladium. This is also one of the few metals that do not brittle and keeps to a large extent its original structural properties upon dissolving large amounts of hydrogen. We will therefore mainly focus on palladium. Right after absorption of hydrogen on the metal's surface, diffusion into the metal first requires the dissociation of H_2 into H-atoms, followed by surface diffusion of the atoms in order to find the appropriate locations to enter the metal crystal, after which diffusion into the bulk of the metal occurs. Dissolving hydrogen changes the lattice spacing of the crystal, mechanical stresses and crystal defects may be created, which both affect the diffusive properties of the H-atoms. Needless to say that a detailed discussion of all these complications can not be covered in this section. In the following we will briefly discuss the most important features of hydrogen-metal systems, and discuss diffusion from the gas phase into the metal on the basis of a simple diffusion model that accounts for crossing the surface of the metal. Besides transferring hydrogen into a metal by exposure to hydrogen gas, other methods can be used, like electrochemical deposition or by partially ionizing the gas phase, which circumvent the necessary dissociation after absorption to the metal's surface.

Let us first consider the phase behaviour of the hydrogen/palladium system. For low concentrations of hydrogen, it is homogeneously distributed within the palladium. For large concentrations, and sufficiently low temperatures, where the H-atoms strongly interact (through the crystal environment), phase separation is observed where a H-rich phase coexists with a H-poor phase. In both phases the hydrogen is disordered,while at room temperature the crystal lattice spacing for the H-poor phase is $0.3894\,nm$, and for the H-rich phase $0.4040\,nm$ [15, 16]. It seems likely that this phase equilibrium is similar to a gas-liquid phase coexistence, where "the gas" is the H-poor phase, and "the liquid" is the H-rich phase. The only difference between the two phases is their hydrogen concentration (and the difference lattice spacing of the palladium crystal), without any structural differences, like for a gas and a liquid. The experimental phase diagram is shown in Fig.8a [17, 18]. The line is the binodal, which has much the same form as for common gas-liquid coexistence. Notice that large amounts of hydrogen can be solved in palladium, where the ratio of hydrogen to palladium atoms is close to unity.

The simplest way to dissolve hydrogen in metals (palladium in particular), is by exposing the metal to gaseous hydrogen, of which the pressure can be varied by external means. Typically, more hydrogen dissolves when the hydrogen pressure is increased. First consider small pressures, such that H_2-molecules in the gaseous phase and H-atoms in the palladium environment do not interact with each other. For such ideal systems the chemical potential μ_g and μ_{Pd} of hydrogen in the gaseous phase and in palladium, respectively, depend on the corresponding

number concentrations ρ_g and ρ_{Pd} as,

$$\begin{aligned} \mu_g &= \mu_g^0(T) + k_B T \, \ln\{\Lambda^3 \, \rho_g\} \, , \\ \mu_{Pd} &= \mu_{Pd}^0(T) + k_B T \, \ln\{\Lambda^3 \, \rho_{Pd}\} \, , \end{aligned} \tag{60}$$

where $\mu_g^0(T)$ and $\mu_{Pd}^0(T)$ depend on temperature T only, and Λ is the Broglie wave length. Since an H_2-molecule splits in two H-atoms on dissolving in palladium, in equilibrium we have,

$$\mu_g \; = \; 2 \, \mu_{Pd} \, , \tag{61}$$

and hence,

$$\rho_{Pd} \; = \; f(T) \, \sqrt{p} \, , \tag{62}$$

where we used the ideal gas law $p = k_B T \, \rho_g$ for the pressure of the gaseous hydrogen phase, and where,

$$f(T) \; = \; \left[\, \frac{\Lambda^{-3}}{k_B T} \, \exp\left\{ \frac{\mu_g^0(T) - 2 \, \mu_{Pd}^0(T)}{k_B T} \right\} \right]^{1/2} \, , \tag{63}$$

is a function of temperature. That the amount of hydrogen that dissolves varies linearly with the square root of the pressure is commonly referred to as Sieverts's law [20]. Sieverts's law is verified experimentally, as can be seen in Fig.8b (for the $V_3 \, Ga \, H_x$-system). For higher pressures there are strong deviations from Sievert's law due to interactions between hydrogen molecules/atoms, as can be seen from Fig.8c [19]. Also note that more hydrogen dissolves at lower temperatures. Since diffusion typically slows down at lower temperatures, their are optimum operation conditions where a compromise must be found between appropriate time scales for hydrogen loading/recovery and the amount of hydrogen that can be stored.
Diffusion of hydrogen atoms within the bulk of the metal is described by Fick's law (46). The above mentioned changes in metal structure upon dissolving hydrogen can lead to a position dependent diffusion coefficient, or alternatively, to a contribution to the flux that relates to stresses that result from the crystal structure deformation. These effects will be neglected in the following. The diffusion of H_2-molecules in the gas phase is assumed to be sufficiently fast as compared to transfer rates to the metal, so that the concentration within the gas phase is a constant, independent of position. We will also assume that the hydrogen concentration in the gas is independent of time (which is the case when the gas container is very large compared to the volume of the metal, and/or when gas is conti nuously supplied). A complication that needs to be considered here is the above described processes that occur right after absorption of H_2-molecules onto the metal's surface. A detailed account of these surface processes is far beyond the scope of this chapter. Here, we simply lump all these processes in an energy barrier within a narrow region at the metal's surface that each molecule has to overcome on transfer from the gas phase to the metal bulk. The height of this barrier sets the ratio between the time-independent concentrations at the metal's surface on the gas-phase side and the metal-bulk side (see the sketch in Fig.9a). The surface-concentration ratio is proportional to $\exp\{-\beta \, E_b\}$, where E_b is the height of the energy barrier. The calculation of this energy is a complicated problem in itself, depending on all the complicated surface processes described above. We will refrain from considering these surface processes, and simply assume the concentration at the

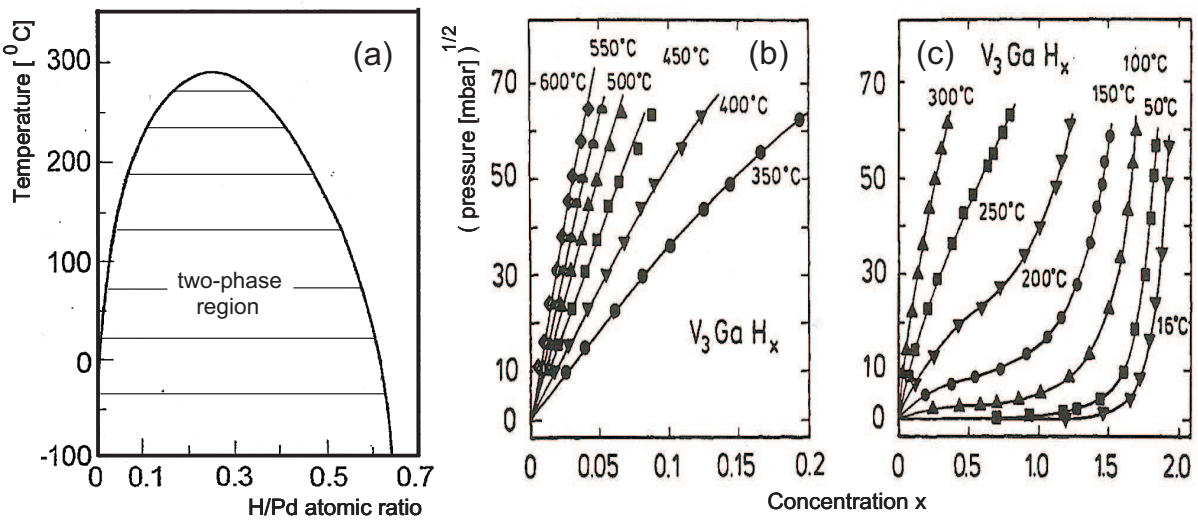

Fig. 8: *(a) The phase diagram of hydrogen/palladium. The solid line is the binodal corresponding to the coexistence between a H-rich and H-poor phase, of course both embedded within the palladium (taken from Ref.[17]). (b) The amount of dissolved hydrogen in the $V_3\,Ga\,H_x$-system for low pressures, and (c) for high pressures (taken from Ref.[19]).*

metal's surface, just inside the bulk, to be a given constant ρ_0^*. The diffusion process is thus described by the equations,

$$\begin{aligned} \frac{\partial}{\partial t}\,\rho(z,t) &= D\,\frac{\partial^2}{\partial z^2}\,\rho(z,t) \quad , \quad z>0\;,\; t>0\;, \\ \rho(z=0,t) &= \rho_0^* \quad , \quad t>0\;, \\ \rho(z,t=0) &= 0 \quad , \quad z>0\;. \end{aligned} \tag{64}$$

where z is the perpendicular distance from the metal's surface (as depicted in Fig.9a). The middle boundary condition states that the concentration at the surface is always equal to ρ_0^*, and the last initial condition ensures that the starting situation (at time $t=0$) is one where there is no hydrogen within the metal. The solution of this set of equations is,

$$\rho(z,t) \;=\; \rho_0^*\,\mathit{erfc}\left\{\frac{z}{\sqrt{4\,D\,t}}\right\}\;, \tag{65}$$

where "*the complementary error-function*" is defined as,

$$\mathit{erfc}\{x\} \equiv \frac{2}{\sqrt{\pi}}\int_x^\infty dw\,\exp\{-w^2\}\;. \tag{66}$$

These theoretical concentration profiles are plotted in Fig.9b. Obviously, the concentration profile spreads into the palladium as time evolves. In these plots, the value of the diffusion coefficient is taken equal to its typical value $D=10^{-7}\,m^2/s$. The total amount of hydrogen that diffused into the palladium at a certain time t is equal to,

$$\Delta\rho(t) \;=\; A\int_0^\infty dz\,\rho(z,t) \;=\; 4\,A\,\rho_0^*\,\sqrt{\frac{D\,t}{\pi}}\;, \tag{67}$$

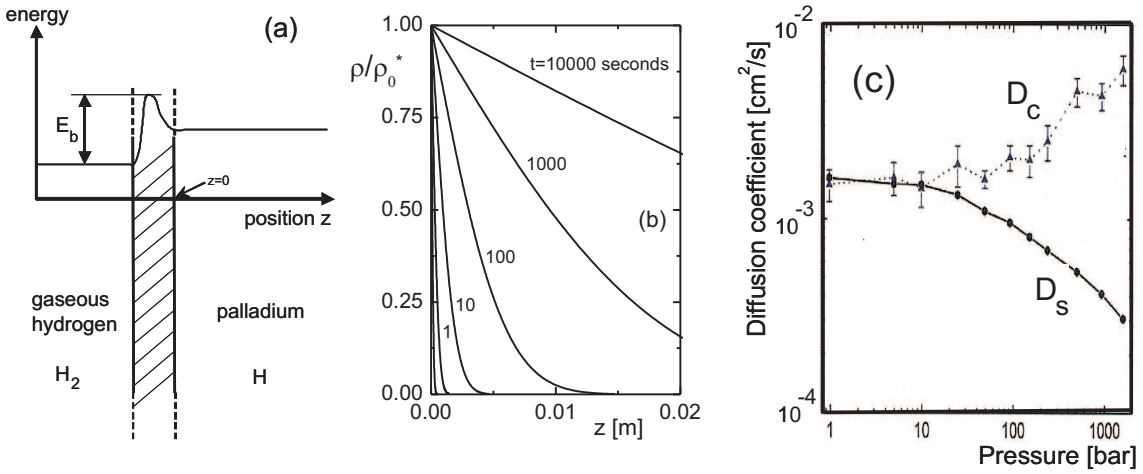

Fig. 9: *(a) A sketch of the simplified model for the kinetics of transfer of hydrogen from the gas phase to the metal bulk. (b) The concentration profiles (ρ/ρ_0^* versus z) for different times, according to eqs.(65,66) The value of the diffusion coefficient is taken equal to $D = 10^{-7}\ m^2/s$. (c) The self- and collective diffusion coefficients of hydrogen in $Zn(bdc)(ted)_{0.5}$, $bdc =$ benzenedicarboxylate, $ted =$ triethylenediamine (taken from Ref.[21]).*

where A is the area of the surface that is exposed to the hydrogen gas. The amount of stored hydrogen thus saturates as the square root of time. Typically, a palladium with a surface area of $A = 1\,m^2$ stores within an hour about $0.04 \times \rho_0^*[m^{-3}]$ hydrogen atoms. A reasonable estimate for ρ_0^* is a typical concentration in equilibrium, which is of the order $10^{27}\ H - atoms/m^3$. This gives an amount of hydrogen stored in one hour equal to about $100\,gram$. It is questionable whether this slow storage rate justifies an economic application, also in view of the high price of palladium [I am, however, hesitant to make a statement like this since my knowledge of economy is essentially equal to zero].

Both the self- and collective diffusion coefficients of hydrogen atoms are concentration dependent as a result of mutual interactions. This can be seen in Fig.9c, where both coefficients are plotted as a function the pressure of the gas phase for a certain metallic compound [21]. As explained in the introduction to section 3, the expected increase of the collective diffusion coefficient and the decrease of the self diffusion coefficient in case of repulsive $H - H$ interactions with increasing concentration is indeed observed. For larger concentrations of hydrogen and sufficiently low temperatures, however, attractions between H-atoms must be present since a gas-liquid phase separation is observed, as discussed above. Since gas-liquid phase transitions are abundant and occur in many different types of systems, the next section is devoted to the kinetics of gas-liquid phase separation from an initially unstable state, which is referred to as spinodal decomposition.

Solutions of Fick's diffusion equation for many types of geometries (like the infinite half-plane geometry in the above example) are discussed in Ref.[22].

4 A Negative Diffusion Coefficient: Spinodal Decomposition

As already mentioned at the end of the introduction to section 3, the collective diffusion coefficient can become negative when strong attractions between the molecules exist. This leads to a temporal increase of inhomogeneities (which are always present due to fluctuations) and ultimately leads to full phase separation. According to eq.(59) the collective diffusion coefficient is negative when $dP^{eq}/d\bar{\rho} < 0$ (with P^{eq} the equilibrium pressure of the homogeneous system and $\bar{\rho}$ the number density of the homogeneous system). The pressure thus decreases with increasing concentration, which is counter intuitive, and therefore hints to an instability. The kinetics of phase separation starting from an homogeneous, unstable system is referred to as **spinodal decomposition**. Phase separation from an initially meta-stable system, where nuclei are formed that grow in time, is referred to as **nucleation-and growth**. As will be seen in this section, the initial morphology in case of spinodal decomposition is qualitatively different from nucleation and growth. Instead of more-or-less ad-random distributed small nuclei of a significantly different concentration as compared to the initially homogeneous system, during spinodal decomposition a continuous growth of density differences is observed, where the relatively low and high concentration regions form a bi-continuous, space-spanning labyrinth structure.
The aim of this section is to quantitatively describe the temporal evolution of the density during the initial stages of phase separation of an unstable, initially homogeneous state. The point of departure is the generalized diffusion equation (52). This approach can be considered as the microscopic foundation of the classic **Cahn-Hilliard theory of spinodal decomposition**, which is based on irreversible thermodynamics [23, 24, 25].

4.1 An introduction to spinodal decomposition

Consider a homogeneous system that is unstable. In an experiment such a system may be prepared by suddenly cooling the system from a temperature in the stable region in the phase diagram to a temperature in the unstable part, where $dP^{eq}/d\bar{\rho} < 0$. Such a sudden change is commonly referred to as *a quench*. Macroscopic density inhomogeneities develop after the quench. The temporal evolution of the density is sketched in Fig.10. The inhomogeneous density can be thought of as being a superposition of sinusoidal density variations (in mathematical terms this refers to Fourier decomposition). A sinusoidally varying density is referred to as *a density wave*. As will be seen later in this section, during the initial stages of the phase separation, one of these density waves grows most fast. The wavelength corresponding to this most fast growing density wave is typically of a macroscopic size, of the order of hundreds of microns. In the *initial stage* of the phase separation, therefore, both the change $\delta\rho$ of the density and gradients of the density are small, as sketched in Fig.10 (upper panel). The initial stage is also referred to as the *linear regime*, since equations of motion for the density may be linearized with respect to $\delta\rho$. Then there is the so-called *intermediate stage*, where $\delta\rho$ is not small anymore, so that linearization is no longer allowed. Gradients of the density are still small, like in the initial stage, due to the long wavelengths that are unstable. This stage is depicted in Fig.10 in the second upper panel. Subsequently, the decomposition reaches the so-called *transition stage* where the lower and larger binodal concentrations ($\bar{\rho}_-$ and $\bar{\rho}_+$, respectively) are attained in various parts of the system, as sketched in Fig.10, the second lower panel. These binodal concentrations are the concentrations of the two phases that coexist when phase separation is completed. At this transition stage, sharp interfaces between the regions with concentrations close to $\bar{\rho}_-$ and $\bar{\rho}_+$ exist. Inhomogeneities are now large, and higher order terms in gradients

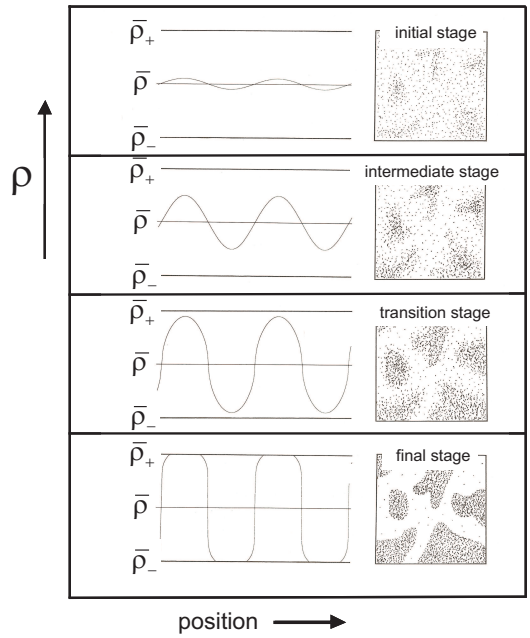

Fig. 10: *A sketch of the temporal development of the density after a quench into the unstable part of the phase diagram. Time increases from top to bottom. The left column of figures is a sketch of the density versus position, while the right column depicts a corresponding morphology of density variations. The concentrations $\bar{\rho}_+$ and $\bar{\rho}_-$ are the binodal concentrations, which are the concentrations of the two coexisting phases after phase separation is completed. Taken from Ref.[12].*

of the density come into play. In the *late stage* of the phase separation the interfaces develop : concentration gradients sharpen and the interfacial curvatures change to ultimately establish coexistence (see Fig.10, lower panel). We thus arrive at the following classification of the different stages during decomposition,

$$
\begin{aligned}
Initial\ stage \ &: \ \delta\rho/\bar{\rho}\ is\ small, \\
&\quad gradients\ are\ small\ (\text{"}diffuse\ interfaces\text{"}), \\
\\
Intermediate\ stage \ &: \ \delta\rho/\bar{\rho}\ is\ not\ small, \\
&\quad gradients\ are\ small\ (\text{"}diffuse\ interfaces\text{"}), \\
\\
Transition\ stage \ &: \ \delta\rho/\bar{\rho}\ is\ large, \\
&\quad gradients\ are\ not\ small\ (\text{"}sharp\ interfaces\text{"}), \\
\\
Final\ stage \ &: \ \delta\rho/\bar{\rho}\ is\ large, \\
&\quad gradients\ are\ large\ (\text{"}very\ sharp\ interfaces\text{"}).
\end{aligned}
$$

The terminology (i) "small", (ii) "not small" and (iii) "large" means that equations of motion for the density can be expanded (i) to leading order, (ii) to second order and (iii) all orders must be accounted for. Equations of motion for the density in the initial and intermediate stage can be expanded to leading order with respect to gradients of the density, while the leading non-linear contributions in $\delta\rho/\bar{\rho}$ must be included in the intermediate stage. The second order terms in

an expansion with respect to gradients of the density, which must be included in the transition stage, are referred to here as describing the dynamics of *sharp interfaces*, while all higher order terms must be included to realistically describe the dynamics of *very sharp interfaces* in the final stage. These very sharp interfaces have a width of the order of a few molecule diameters (except in case of quenches very close to the critical point, where the equilibrium interfacial thickness may be large).

4.2 Spinodal decomposition in the initial stage

In this section we describe the initial stage of demixing quantitatively, where the formation of inhomogeneities is a diffusive process. As before, let $\bar{\rho}$ denote the number density of colloidal particles in the homogeneous state, before decomposition occurred, and let $\rho(\mathbf{r},t)$ denote the macroscopic number density as a function of the position $\mathbf{r}$ in the system at time t after the system became unstable and started to demix. Define the change of the macroscopic density $\delta\rho(\mathbf{r},t)$ relative to that in the homogeneous state as,

$$\rho(\mathbf{r},t) \;=\; \bar{\rho} + \delta\rho(\mathbf{r},t)\;. \tag{68}$$

In the initial stage of the phase separation we have,

$$\frac{\mid \delta\rho(\mathbf{r},t)\mid}{\bar{\rho}} \;\ll\; 1\;, \tag{69}$$

allowing linearization of the generalized diffusion equation (52) with respect to the change $\delta\rho$ of the density.
Let δg denote the accompanied change of the pair-correlation function,

$$g(\mathbf{r},\mathbf{r}',t) \;=\; g_0(\mid \mathbf{r}-\mathbf{r}'\mid) \;+\; \delta g(\mathbf{r},\mathbf{r}',t)\;. \tag{70}$$

Here, g_0 is the pair-correlation function of the homogeneous system right after the quench, before phase separation occurred. To obtain a closed equation for $\delta\rho$, the change δg of the pair-correlation function must be expressed in terms of $\delta\rho$. Such a *closure relation* may be obtained as follows. An important feature is that the pair-correlation function in the integral in the diffusion equation (52) is multiplied by the pair-force $\nabla V(\mid \mathbf{r}-\mathbf{r}'\mid)$, so that a closure relation is only needed for small distances $\mid \mathbf{r}-\mathbf{r}'\mid \leq R_V$, with R_V the range of the pair-interaction potential. R_V is usually of the order of the size of the molecules. Relaxation of density variations over such small distances is much faster than the demixing rates of the very long unstable wavelengths, simply because it takes more time to displace colloidal particles over larger distances. On a coarsened time scale that is much larger than relaxation times of inhomogeneities that extend over distances of the order R_V, but which still resolves the phase separation process, the pair-correlation function in the integral in the generalized diffusion equation may be replaced by the equilibrium pair-correlation function. This is the statistical equivalent of the **thermodynamic local-equilibrium approximation**. The equilibrium pair-correlation function is to be evaluated at the instantaneous macroscopic density in between the positions $\mathbf{r}$ and $\mathbf{r}'$ (compare to what has been done in subsection 3.2). Hence, to first order in $\delta\rho$, and for $\mid \mathbf{r}-\mathbf{r}'\mid \leq R_V$,

$$\delta g(\mathbf{r},\mathbf{r}',t) = \delta g^{eq}(\mid \mathbf{r}-\mathbf{r}'\mid)\Big|_{density=\rho(\frac{\mathbf{r}+\mathbf{r}'}{2},t)} = \frac{dg^{eq}(\mid \mathbf{r}-\mathbf{r}'\mid)}{d\bar{\rho}}\,\delta\rho(\tfrac{\mathbf{r}+\mathbf{r}'}{2},t)\,, \tag{71}$$

and,

$$g_0(|\,\mathbf{r}-\mathbf{r}'\,|) \;=\; g^{eq}(|\,\mathbf{r}-\mathbf{r}'\,|)\,, \tag{72}$$

where g^{eq} is the equilibrium pair-correlation function for a homogeneous system with density $\bar{\rho}$ and the temperature after the quench. The two relations (71,72) are certainly wrong for distances $|\,\mathbf{r}-\mathbf{r}'\,|$ comparable to the wavelengths of the unstable density variations. For such distances the system is far out of equilibrium. The validity of the relations (71,72) is limited to small distances, where $|\,\mathbf{r}-\mathbf{r}'\,|\leq R_V$. Substitution of eqs.(71,72) into the generalized diffusion equation (52), renaming $\mathbf{R}=\mathbf{r}'-\mathbf{r}$, yields,

$$\begin{aligned}\frac{\partial}{\partial t}\,\delta\rho(\mathbf{r},t) \;&=\; D_c^0\,\Big\{\,\nabla^2\delta\rho(\mathbf{r},t)-\beta\,\bar{\rho}\,\nabla\cdot\int d\mathbf{R}\,[\nabla_R V(R)] \\ &\qquad\times\left(g^{eq}(R)\,\delta\rho(\mathbf{r}+\mathbf{R},t)+\bar{\rho}\,\frac{dg^{eq}(R)}{d\bar{\rho}}\,\delta\rho(\mathbf{r}+\tfrac{1}{2}\mathbf{R},t)\right)\Big\}\,,\end{aligned} \tag{73}$$

with ∇_R the gradient operator with respect to $\mathbf{R}$. The density can now be gradient-expanded like in subsection 3.2. We now need to extend the expansion to include the two higher order terms as compared to that in eq.(53), for reasons that will become clear in a moment. For example,

$$\begin{aligned}\rho(\mathbf{r}+\mathbf{R},t) \;&\approx\; \rho(\mathbf{r},t)+\mathbf{R}\cdot\nabla\rho(\mathbf{r},t) \\ &\qquad +\tfrac{1}{2}\,\mathbf{RR}:\nabla\nabla\rho(\mathbf{r},t)+\tfrac{1}{6}\,\mathbf{RRR}\,\vdots\,\nabla\nabla\nabla\rho(\mathbf{r},t)\,,\end{aligned} \tag{74}$$

where the vertical dots indicate contraction of adjacent indices (for example, $\mathbf{RR}:\nabla\nabla=\sum_{m,n=1}^{3}R_mR_n\nabla_n\nabla_m$). A similar expansion is made for $\rho(\mathbf{r}+\frac{1}{2}\mathbf{R},t)$. Substitution into eq.(73), noting that $[\nabla_R V(R)]=(\mathbf{R}/R)\;dV(R)/dR$, and integration with respect to the directions of $\mathbf{R}$, and using eqs.(56) together with,

$$\begin{aligned}\oint d\hat{\mathbf{R}}\;\hat{\mathbf{R}}\,\hat{\mathbf{R}}\,\hat{\mathbf{R}}\,\hat{\mathbf{R}} \;&=\; \mathbf{0}\,, \\ \oint d\hat{\mathbf{R}}\;\hat{\mathbf{R}}_i\,\hat{\mathbf{R}}_j\,\hat{\mathbf{R}}_m\,\hat{\mathbf{R}}_m \;&=\; \frac{4\pi}{15}\,[\,\delta_{ij}\,\delta_{mn}+\delta_{im}\,\delta_{jn}+\delta_{in}\,\delta_{mi}\,]\,,\end{aligned} \tag{75}$$

where δ_{ij} is the Kronecker delta, leads to, with some effort,

$$\frac{\partial\rho(\mathbf{r},t)}{\partial t} \;=\; D_c^0\left[\,\beta\,\frac{dP^{eq}}{d\bar{\rho}}\,\nabla^2\rho(\mathbf{r},t)+\Sigma\,\nabla^2\nabla^2\rho(\mathbf{r},t)\right]\,. \tag{76}$$

This equation of motion reproduces Fick's diffusion equation with the expression (59) for the collective diffusion coefficient, but with an additional contribution $\sim\nabla^2\nabla^2\rho$, with a proportionality factor equal to,

$$\Sigma \;=\; \frac{2\pi}{15}\,\bar{\rho}\int_0^\infty dR\,R^5\,\frac{dV(R)}{dR}\left(g^{eq}(R)+\frac{1}{8}\,\bar{\rho}\,\frac{dg^{eq}(R)}{d\bar{\rho}}\right)\,. \tag{77}$$

This constant is commonly referred to as **the Cahn-Hilliard square-gradient coefficient**. This higher order gradient contribution to Fick's diffusion equation is insignificant for stable systems, where $dP^{eq}/d\bar{\rho}>0$. For unstable systems where $dP^{eq}/d\bar{\rho}<0$, on the contrary, this contribution is essential, as will be seen shortly.

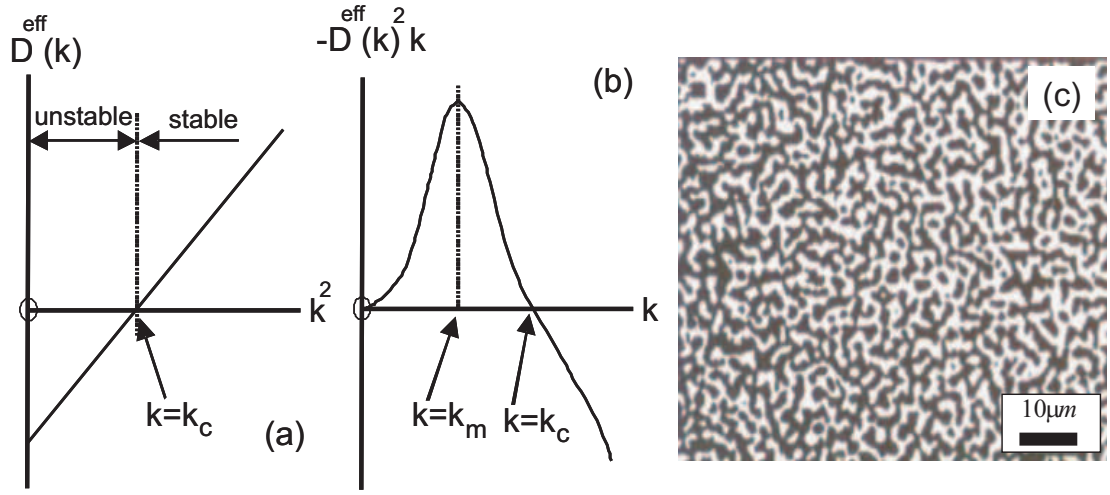

Fig. 11: *(a) The effective diffusion coefficient as a function of the wave vector. The critical wave vector k_c separates the unstable from the stable wave vectors. (b) The demixing rate as a function of the wave vector. k_m is the wave vector for which the corresponding density wave grows most fast. (c) The typical bi-continuous interconnected labyrinth structure of low (bright regions) and higher (dark regions) density that exists during the initial stages of spinodal demixing. This picture is taken from Ref.[26]*

An arbitrary spatially varying density can be decomposed in a sum of sinusoidal density variations with varying wave lengths. It thus suffices to consider the same initial sinusoidal density variation $\rho(\mathbf{r}, t=0) = \bar{\rho} + \delta\rho_0 \times \sin\{\mathbf{k}\cdot\mathbf{r}\}$ (as already introduced at the end of the introduction of section 3) where $\Lambda = 2\pi/k$ is the wavelength of the *density wave*, and the direction of the *wave vector* $\mathbf{k}$ defines the direction in which the density wave extends. Substitution of the Ansatz $\rho(\mathbf{r}, t) = \bar{\rho} + \delta\rho(t) \times \sin\{\mathbf{k}\cdot\mathbf{r}\}$ into eq.(76) immediately gives,

$$\delta\rho(t) \;=\; \delta\rho_0 \,\exp\left\{-D^{eff}(k)\,k^2\,t\,\right\}\;, \tag{78}$$

where the *effective diffusion coefficient* is equal to,

$$D^{eff}(k) \;=\; D_c^0\,\beta\left[\frac{dP^{eq}}{d\bar{\rho}} + \Sigma\,k^2\right]\;. \tag{79}$$

It follows from eq.(78) that the sinusoidal density variations for which $D^{eff}(k) < 0$ are unstable. For most systems $\Sigma > 0$, so that it follows from eq.(79) that there are unstable modes only when $dP^{eq}/d\bar{\rho} < 0$, which reproduces the classic thermodynamic instability criterion. Furthermore, only sufficiently small wave vectors are unstable and contribute to demixing. According to eq.(79) all wave vectors smaller than the critical wave vector,

$$k_c \;=\; \sqrt{-\frac{dP^{eq}/d\bar{\rho}}{\Sigma}}\;, \tag{80}$$

are unstable. That is, sinusoidal density variations with a wavelength larger than $\Lambda_c = 2\pi/k_c$ will grow in amplitude, giving rise to the creation of inhomogeneities. Density variations with a shorter wavelength remain stable (see Fig.11a). This is consistent with the assumption made in the above analysis that only long wavelengths (much larger than $2\pi/R_V$) are unstable.

Note that when the higher order spatial derivatives in the diffusion equation (76) (corresponding to the contribution $\sim \Sigma$ in eq.(79) for the effective diffusion coefficient) are omitted for unstable systems, arbitrary short wavelength density variations demix arbitrary fast. This is clearly unphysical, so that the higher order spatial derivatives are essential for a realistic description of demixing, contrary to the diffusion in stable systems.
The rate with which density variations grow, according to eq.(78), is equal to $-D^{eff}(k)\,k^2$. For,

$$k_m \;=\; \sqrt{-\frac{dP^{eq}/d\bar{\rho}}{2\Sigma}} \;=\; k_c/\sqrt{2}\;, \tag{81}$$

the growth rate attains a maximum value (see Fig.11b). The amplitude of the density variation with a wavelength equal to $\Lambda_m = 2\pi/k_m$ thus grows faster than any other demixing density wave. This introduces a characteristic length scale of inhomogeneities. Since the growth rates are independent of the direction of the wave vector, a bi-continuous interconnected labyrinth structure of low and higher density exists during the initial stages of demixing. A sketch of such a labyrinth structure is given in Fig.11c. The width of the labyrinth substructures are equal to the wavelength Λ_m of the most fast growing density wave.

4.3 The microscopic origin of the spinodal instability

To understand on a microscopic level why a system can become thermodynamically unstable, let us rewrite the generalized diffusion equation (52) as,

$$\frac{\partial}{\partial t}\,\delta\rho(\mathbf{r},t) \;=\; -\beta\,D_c^0\,\nabla\cdot\rho(\mathbf{r},t)\,\left[\mathbf{F}^{Br}(\mathbf{r},t)+\mathbf{F}^{Int}(\mathbf{r},t)\right]\;, \tag{82}$$

where,

$$\mathbf{F}^{Int}(\mathbf{r},t) \;=\; -\int d\mathbf{r}'\;g(\mathbf{r},\mathbf{r}',t)\,\rho(\mathbf{r}',t)\,\nabla V(|\,\mathbf{r}-\mathbf{r}'\,|)\;, \tag{83}$$

is the direct force, which stems from inter-molecular potential interactions (as specified by the pair-potential V) and,

$$\mathbf{F}^{Br}(\mathbf{r},t) \;=\; -k_BT\,\nabla\ln\{\rho(\mathbf{r},t)\}\;, \tag{84}$$

is the Brownian force on a molecule at the position $\mathbf{r}$. Now consider a molecule at $\mathbf{r}$ in an inhomogeneous environment, as sketched in Fig.12a. The inhomogeneous macroscopic density may be thought of as an instantaneous realization of the fluctuating density. A little thought shows that the Brownian force is always directed towards the region with lower concentration, as depicted in Fig.12a. Now suppose that the pair-interaction potential is purely attractive. The direct force $\mathbf{F}^{Int}$ is then directed in the opposite direction, towards the region with a larger density, since in that region there are more neighbouring molecules attracting the molecule under consideration : this can also be seen formally from eq.(83) for the direct force, using a purely attractive pair-interaction potential. On lowering the temperature, the Brownian force diminishes, since that force is directly proportional to the temperature. The direct force, however, increases in magnitude, due to the fact that the pair-correlation function becomes more pronounced (to leading order in the density this follows from the expression $g = \exp\{-V/k_BT\}$, where $V<0$ for an attractive pair-potential). At the temperature where $|\,\mathbf{F}^{Int}\,| > |\,\mathbf{F}^{Br}\,|$, the net force on the molecule is directed towards the region with a larger density. This is the mechanism that is responsible for **uphill diffusion**, and leads to phase separation.

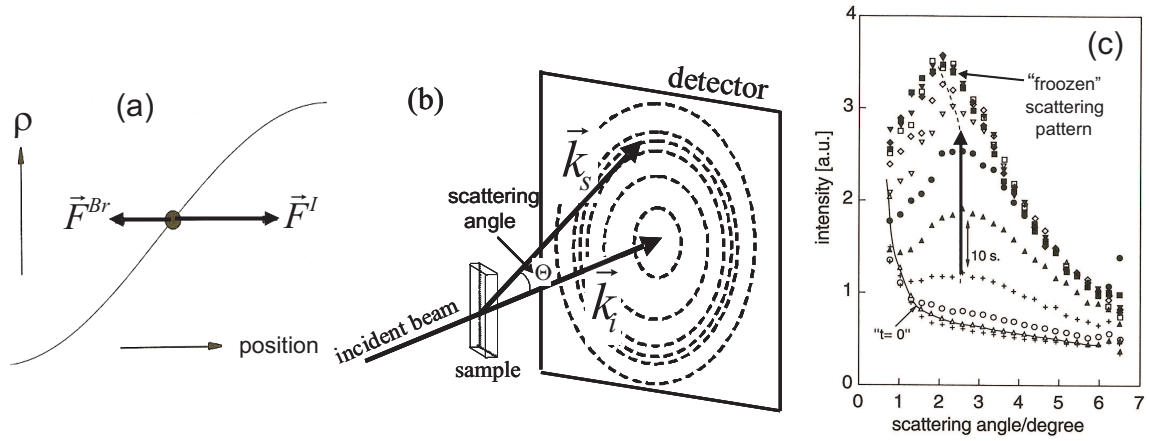

Fig. 12: *(a) The direct and Brownian force on a molecule, indicated by •, in an inhomogeneous system. For an attractive direct force* $\mathbf{F}^I$*, its direction is towards the region with larger concentration, as sketched here. (b) A schematic of the scattering set up. The wave vector is the equal to* $\mathbf{k}_s - \mathbf{k}_i$*, with* $\mathbf{k}_s$ *the scattered wave vector and* $\mathbf{k}_i$ *the incident wave vector, which both have a length equal to* $2\pi/\lambda$*, where* λ *is the wavelength of the light beam. (c) The scattered intensity from a suspension of stearyl-coated silica particles as a function of the scattering angle. Each curve is measured* 10 *seconds after each other. At later times, the scattering peak "freezes", due to the formation of a gel in the regions of higher concentration. From Ref.[27].*

4.4 A light scattering experiment

The above predictions can be verified by means of time resolved light scattering. It can be shown that the time-dependent scattered intensity $I(t)$ at very small scattering angles from an inhomogeneous system is given by (see, for example, Ref.[12]),

$$I(k,t) \ \sim <|\,\delta\rho(\mathbf{k},t)\,|^2> \ , \tag{85}$$

where the brackets $< \cdots >$ refer to ensemble averaging over initial conditions. The wave vector can be varied through variation of the scattering angle Θ (the angle between the incident beam and the direction of detection: see Fig.12b)). In case of scattering, the wave vector is equal to $\mathbf{k} = \mathbf{k}_s - \mathbf{k}_i$, where $\mathbf{k}_i$ and $\mathbf{k}_s$ point in the direction of the incident beam and the direction of detection, respectively. In case of elastic scattering, both the incident and scattered wave vector $\mathbf{k}_s$ and $\mathbf{k}_i$ have the same length equal to $2\pi/\lambda$, where λ is the wavelength of the light. It follows that $k = \frac{4\pi}{\lambda}\sin\{\Theta/2\} \approx \frac{2\pi}{\lambda}\,\Theta$, for small scattering angles Θ. The wave vector thus determines the position on a screen at which scattered light is collected, as sketched in Fig.12b. Substitution of eq.(78) into eq.(85) gives,

$$I(k,t) \ \sim < \delta\rho_0^2 > \ \exp\left\{-2\,D^{eff}(k)\,k^2\,t\right\} \ . \tag{86}$$

This result predicts that in the initial stage of decomposition, $\ln\{I(k,t)\}$ is a linear function in time and that the intensity develops a "ring-like scattering pattern", where the position of the peak grows at a time-independent position. This is indeed observed in some systems, like in dispersions of stearyl silica colloidal particles [27]. As can be seen from the plots in Fig.12c, the ring-like scattering pattern for this particular system "freezes" at some time during demixing. This is due to the formation of a gel-like phase in the more concentrated region of the labyrinth structure. In other systems (see, for example, Refs.[28, 29]), the peak position of the scattering

ring is observed to shift to lower scattering angles right from the start of the experiment. Such a shift of position of the peak of the ring-like scattering pattern is expected in the intermediate stage of demixing (the above analysis has been extended to include the intermediate stage in Refs.[12, 30]). Probably the time range within which the linear theory applies is already past at the time a first reliable measurement could be performed.
Spinodal decomposition is also found for hydrogen dissolved in palladium, within the two-phase region in Fig.8a. The required attractive interactions between the H-atoms is probably due to palladium-crystal-environment mediated interactions.

References

[1] R. Festa, E. Galleani d'Agliano, Physica A **90**, 229 (1978)

[2] L. Gunther, M. Revzen, A. Ron, Physica A **95**, 367 (1979)

[3] M.P. Lettinga, E. Grelet, Phys. Rev. Lett. **99**, 197802 (2007)

[4] E. Pouget, E. Grelet. M.P. Lettinga, Phys. Rev. E **84**, 041704 (2011)

[5] C. Dalle-Ferrier, M. Krüger, R.D.L. Hanes, S. Walta, M.C. Jenkins, S.U. Egelhaaf, Soft Matter **7**, 2064 (2011)

[6] K. Kang, J.K.G. Dhont, J. Chem. Phys. **122**, 044905 (2005)

[7] K. Kang, J.K.G. Dhont, J. Chem. Phys. **124**, 044907 (2006)

[8] K. Kang, J.K.G. Dhont, J. Chem. Phys. **126**, 214501 (2007)

[9] P.-G. de Gennes, J. Chem. Phys. **55**, 572 (1971)

[10] K.E. Evans, S.F. Edwards, J. Chem. Soc., Faraday Trans. **2**, 1891 (1981)

[11] D. Richter, M. Monkenbusch, A. Arbe, J. Colmenero, Adv. Polym. Sci. **174**, 1-221 (2005)

[12] J.K.G. Dhont, *An Introduction to Dynamics of Colloids*, Elsevier, Amsterdam, 1996

[13] G. Nägele, Physics Reports **272**, 215 (1996)

[14] G. Nägele, J.K.G. Dhont, G. Meier, *Diffusion in Condensed Matter*, Chapter 16, page 619, (eds. P. Heitjans, J. Kärger), Springer Verlag, Berlin.

[15] A.J. Maeland, Canadian Journal of Physics **46**, 121 (1968)

[16] T.B. Flanagan, W.A. Oates, Ann. Rev. Mater. Sci. **21**, 269 (1991)

[17] J. Vökl, G. Alefeld, *Diffusion in Solids: Recent Developments*, (eds. A.S. Nowick, J.J. Burton), Academic press, New York,1975

[18] I.S. Anderson, D.K. Ross, C. Carlile, Phys. Lett. **68**A, 249 (1978)

[19] M. Schlereth,H. Wipf, J. Phys.: Condens. Matter **2**, 6929 (1990)

[20] A. Sieverts, Z. Phys. Chemie **88**, 451 (1914)

[21] J. Liu, J.Y. Lee, L. Pan, R.T. Obermyer, S. Simizu, B. Zande, J. Li, S.G. Sankar, J.K. Johnson, J. Phys. Chem. C **112**, 2911 (2008)

[22] J. Crank, *The Mathematics of Diffusion*, Oxford Science Publications, Clarendon Press, Oxford, 1975

[23] J.W. Cahn, J.E. Hilliard, J. Chem. Phys. **28**, 258 (1958), **31**, 688 (1959)

[24] M. Hillert, Acta Metallica **9**, 525 (1961)

[25] J.W. Cahn, J. Chem. Phys. **42**, 93 (1965)

[26] I. Demyanchuk, S.A. Wieczorek, R. Holyst, J. Chem. Phys. **121**, 1141 (2004)

[27] H. Verduin, J.K.G. Dhont, J. Coll. Interf. Sci. **172**, 425 (1995)

[28] F. Mallamace, N. Micali, S. Trusso, S.H. Chen, Phys. Rev. E **51**, 5818 (1995)

[29] P. Wiltzius, F.S. Bates, W.R. Heffner, Phys. Rev. Lett. **60**, 1538 (1988)

[30] J.K.G. Dhont, J. Chem. Phys. **105**, 5112 (1996)